Review of Palaeobotany and Palynology 279 (2020) 104224

Contents lists available at ScienceDirect

Review of Palaeobotany and Palynology

journal homepage: www.elsevier.com/locate/revpalbo

New Jersey's paleoflora and eastern North American climate through Paleogene–Neogene warm phases

Sabine Prader [a,b], Ulrich Kotthoff [a,b,*], David R. Greenwood [c], Francine M.G. McCarthy [d], Gerhard Schmiedl [b,e], Timme H. Donders [f]

[a] Center for Natural History, Hamburg University, Bundesstraße 55, D-20146 Hamburg, Germany
[b] Institute of Geology, University of Hamburg, Bundesstraße 55, D-20146 Hamburg, Germany
[c] Department of Biology, Brandon University, 270 18th Street, Brandon, Manitoba R7A 6A9, Canada
[d] Department of Earth Sciences, Brock University, 1812 Sir Isaac Brock Way, St. Catharines, Ontario L2S 3A1, Canada
[e] Center for Earth System Research and Sustainability, Hamburg University, Bundesstraße 55, D-20146 Hamburg, Germany
[f] Palaeoecology, Department of Physical Geography, Heidelberglaan 2, 3584 CS Utrecht, the Netherlands

ARTICLE INFO

Article history:
Received 3 September 2019
Received in revised form 26 March 2020
Accepted 29 March 2020
Available online 1 April 2020

Keywords:
Palynology
Paleoclimate
Miocene
Oligocene
Fagaceae
Paleovegetation

ABSTRACT

Pollen of middle Oligocene to early Miocene age from core sediments from the New Jersey Shallow Shelf (Atlantic Coastal Plain: IODP-Expedition 313, Site M0027A), was analyzed using light- and scanning electron microscopy, and a pollen-based bioclimatic analysis was performed. The microflora is dominated by *Quercus* pollen. Pollen ornamentations indicate that *Quercus* pollen most likely originated from species of sections *Quercus*, *Lobatae*, *Quercus/Lobatae* and aff. section *Protobalanus*. *Eotrigonobalanus*, an extinct Fagaceae lineage, was present in the coastal plain. Relative abundances of several tree taxa (e.g., *Carya*) did not change significantly between the Oligocene warm phases, but contrast to late middle Miocene (comprising most of the Langhian and Serravallian) records from the same area.

By assigning terrestrial palynomorphs to paleovegetation units, topographic movements of these units were identified. The mesophytic forest was the most widespread and zonal vegetation type in the hinterland through the analyzed interval. Periodic changes in the relative abundances of paleovegetation units suggest altitudinal vegetation movements responding to global climate change. Observed movement signals are generally weak, but increases in bisaccate pollen, representing spread of high- and mid-latitude forest, probably reflect the onset of cold intervals such as cooling phases at ~29.1, ~28.5, and 23.5 Ma. Spread of edaphically controlled forest formations during regression phases also indicates climate change. The onset of the Mi-1 event at ~23.03 Ma is probably reflected by a decrease in pollen-inferred paleotemperatures, although the event itself occurred during a sedimentation hiatus. Pollen-based paleoclimate reconstructions indicate long-term stability in temperature and precipitation within the humid warm temperate zone.

1. Introduction

At the Eocene–Oligocene boundary (EOB) at ~33.7 Ma, global climate began to transform from a greenhouse to an icehouse state (Zachos et al., 2001; Pagani et al., 2005; Eldrett et al., 2009). Various mechanisms are under debate as possible drivers of the large-scale glaciation of Antarctica around the first Oligocene isotopic event (Oi-1 event), including the opening of the Drake Passage (Scher and Martin, 2006), orbital forcing (Coxall et al., 2005), and the decline of atmospheric carbon dioxide concentrations (Pagani et al., 2005), with the latter explanation being favored recently (Goldner et al., 2013). Vegetation changed globally across this transition although more gradually and heterogeneously relative to marine-based reconstructions of global climate (Pound and Salzmann, 2017). The Oligocene is marked by a series of eight unipolar glaciation periods (Pekar et al., 2002) during which Antarctica experienced ice sheet growth, resulting in large glacioeustatic sea level fluctuations (Pekar et al., 2002; Wade and Pälike, 2004; Pälike et al., 2006; Pekar et al., 2006). These oscillations are attributed to insolation changes associated with orbital forcing (Wade and Pälike, 2004; Pälike et al., 2006). The waxings and wanings of the East Antarctic ice sheet (EAIS; Zachos et al., 2001) during the Oligocene were not all of equal magnitude. The strongest glacial episode during this epoch is represented by the Oi-2b event (27.0–26.6 Ma; Pekar et al., 2006; Pälike et al., 2006) which resulted in a glacioeustatic

* Corresponding author at: Center for Natural History, Hamburg University, Bundesstraße 55, D-20146 Hamburg, Germany.
E-mail address: ulrich.kotthoff@uni-hamburg.de (U. Kotthoff).

https://doi.org/10.1016/j.revpalbo.2020.104224
0034-6667/

lowering of ~45 m (Pekar et al., 2002). However, only a few records world-wide (e.g., Prebble et al., 2017; Korasidis et al., 2019) deal with the response of plant cover to Oligocene global climatic oscillations.

The inception of the Miocene isotopic event 1 (Mi-1), the second largest climatic aberration since the Oi-1 event (Lear et al., 2004), coincides with the Oligocene–Miocene boundary (OMB) at 23.03 Ma (Liebrand et al., 2011; Gradstein et al., 2012; Cohen et al., 2016). It represents the first and largest cooling episode of the Miocene with a sea-surface temperature decline of ~2 °C prior to the event (Lear et al., 2004; Mawbey and Lear, 2013). Orbital forcing has been discussed as one possible mechanism behind this global cooling event (Naish et al., 2001; Zachos et al., 2001; Pälike et al., 2006). Atmospheric carbon dioxide levels declined in steps since the late Eocene, probably reaching concentrations near modern values during the late Oligocene (Pagani et al., 2005; Roth-Nebelsick et al., 2014). Kotthoff et al. (2014) showed prominent changes at the OMB, resulting in temperature decline and conifer expansion in the eastern North America.

The equator-to-pole temperature gradient became more pronounced following the Oi-1 event, which resulted in a predominantly temperate climate in mid-latitudes of Northern Hemisphere continents (Hably et al., 2000). This time interval was important for a restructuring of the North American (Graham, 1999) and other floras (e.g., Eldrett et al., 2009; Korasidis et al., 2019). Most records of early Oligocene age from the mid-latitudes of Europe indicate a prevailing broadleaf deciduous vegetation character with intermixed Eocene warm-climate floristic elements like *Eotrigonobalanus* (e.g., Velitzelos et al., 2014). So far, few early Oligocene records are available that outline a more broadleaf evergreen vegetation in which broadleaf deciduous vegetation elements played a subordinate role (Kovar-Eder, 2016). Terrestrial records of the Southern Hemisphere indicate an increase of temperate-climate tree taxa, with *Nothofagus* being the dominant taxon (e.g., Prebble et al., 2017; Korasidis et al., 2019).

Most information about the floristic and climatic history of the Oligocene of North America is derived from deposits of the western (e.g., Grímsson et al., 2016; Meyer and Manchester, 1997) and interior (e.g., Wolfe and Schorn, 1989, 1990) parts of the continent. For the early Oligocene, records from the western part of North America suggest a dominantly temperate climate, documented by predominantly broadleaf deciduous forests with a small portion of broadleaf evergreens in the understorey (Meyer and Manchester, 1997) and persistent single warmth-loving elements characteristic of the Eocene (Grímsson et al., 2016). At the same time, intensifying climatic seasonality triggered the development of open landscapes and dry conifer woodlands in the interior of the country (Wolfe and Schorn, 1989, 1990). By the end of the Oligocene, the prevailing climate supported the formation of open grasslands in the western interior of North America (e.g., Retallack et al., 2004; Strömberg, 2005).

The late Paleogene paleofloristic and terrestrial environment of eastern North America is not well understood due to a scarcity of Oligocene floras (e.g., Frederiksen, 1991), while the Brandon Lignite of Vermont provides data on early middle Miocene vegetation in the northeast (e.g., Tiffney, 1977, 1979; Tiffney and Barghoorn, 1979; Tiffney, 1993, 1994; Tiffney et al., 2018), with additional floras informing on Miocene vegetation in the southeast (e.g., Lott et al., 2019). Terrestrial palynomorphs deposited in marine and continental sediments are well-suited for the reconstruction of paleoclimate (e.g., Eldrett et al., 2009), paleovegetation (e.g., Kmenta and Zetter, 2013) and biogeographic history of a region (e.g., Grímsson et al., 2016). Sediment cores drilled in the framework of the Integrated Ocean Drilling Program (IODP) Expedition (Exp.) 313 to the New Jersey Shallow Shelf (NJSS) provided insights into Oligocene and Miocene terrestrial ecosystem development in mid-latitude eastern North America. The recovered deposits contain generally well preserved marine and terrestrial palynomorphs. Furthermore, a robust age model (Browning et al., 2013) was developed for these cores. The sediments represent intervals from the Oligocene (late Rupelian and late Chattian) and early Miocene. Because global climate changes do not affect all regions at the same scale, biotic responses likely differ from one environment to another (Utescher et al., 2015; Pound and Salzmann, 2017). Climate models indicate more constant conditions for the Atlantic east coast during the Oligocene than for other regions (von der Heydt and Dijkstra, 2006), implying a restricted vegetation turnover for the hinterland.

In these contexts, we have evaluated the regional floristic behaviour of the NJSS hinterland based on a quantitative record of terrestrial palynomorphs and bioclimatic estimates from Site M0027 from IODP Exp. 313. These data provide a detailed insight into a mid-latitude terrestrial system during the middle Oligocene to the early Miocene and document long-term patterns of plant persistence/migration in response to global climate oscillations.

2. Material and methods

2.1. Geological setting

2.1.1. Site M0027: Selection, age model and core sediment description

Our study focuses on sediments from Site M0027 recovered during IODP Exp. 313 to the NJSS. The drilling position of Hole M0027A is at 39°38.046′N and 73°37.301′W, at 33.5 m water depth, and at a site-shoreline distance of 40 km (Fig. 1). Site M0027 is the only one of three recovered sites containing Oligocene sequences (Browning et al., 2013; Miller et al., 2013a, 2013b). The analyzed core sediments were deposited from the middle Oligocene to the early Miocene. The age model is based on calcareous nannofossils, dinoflagellate cysts, planktic diatoms, Sr isotopes, and sequence stratigraphy (Browning et al., 2013; Miller et al., 2013a).

The analyzed core sediments comprise four sequences, which correlate with phases of sea-level high stands, while sea-level lowstands (likely connected to glacial phases) led to decreasing sediment deposition or even to sequence boundaries (Browning et al., 2013).

The sampled part of the Oligocene is not well-resolved in the seismic profile (Browning et al., 2013; Miller et al., 2013a, 2013b), either because of the minimal lithological expression or the increasing burial depth; however, Oligocene sequences were identified via core and log inspections (Browning et al., 2013; Miller et al., 2013a, 2013b). Sequence O3 (617–538.68 mbsf), the oldest analyzed sequence, was deposited between ~29.3 and ~28.2 Ma (late Rupelian/early Chattian; Fig. 2). This sequence contains two very poorly resolved sequence boundaries respectively intrasequence reflectors, which are tied to facies changes: reflector o.1 at 596.3 mbsf (~29.0 Ma) and reflector o.5 at 563.0 mbsf (~28.6 Ma; Miller et al., 2013a). The age uncertainty for this sequence is approximately ~0.5 to ~1 Ma. Sequence O6 (538.68–509 or 515 mbsf) comprises the uppermost part of the Oligocene and the transition to the early Miocene (Chattian/Aquitanian) and is not visible seismically (Browning et al., 2013; Miller et al., 2013a, 2013b). A coring gap between 509 and 515 mbsf impedes giving a precise upper sequence boundary of O3 and the basal sequence boundary of the early Miocene Sequence m6, respectively (Miller et al., 2013a). Miller et al. (2013a) set a synthetic sequence boundary at 510 mbsf. The estimated age of Sequence O6 is best dated to ~23.5 to ~23.0 Ma and respective age uncertainties of ± ~0.25 and ~0.5 Ma. The early Miocene Sequence m6 (509 or 515–494.87 mbsf) covers an age interval of ~20.9 to ~20.7 Ma (Aquitanian). Sequence m5.8 (494.87–361.28) is dated to ~20.1 to ~19.2 Ma (late Aquitanian/early Burdigalian). Ages of the analyzed Miocene Sequences m6 and m5.8 have uncertainties of ~0.5 to ~1 Ma, respectively. All analyzed sequences lie within Lithological Unit VII, comprising coarse-grained to fine-grained sands interbedded with silty clay laminae (Expedition 313 Scientists, 2010).

Reconstructions by Scotese et al. (1988) imply that the NJSS study area was situated ~2° further south during the Oligocene and Miocene, and reached its modern position between 39° and 40°N during the Pliocene. Significant topographic change and significant increase in relief

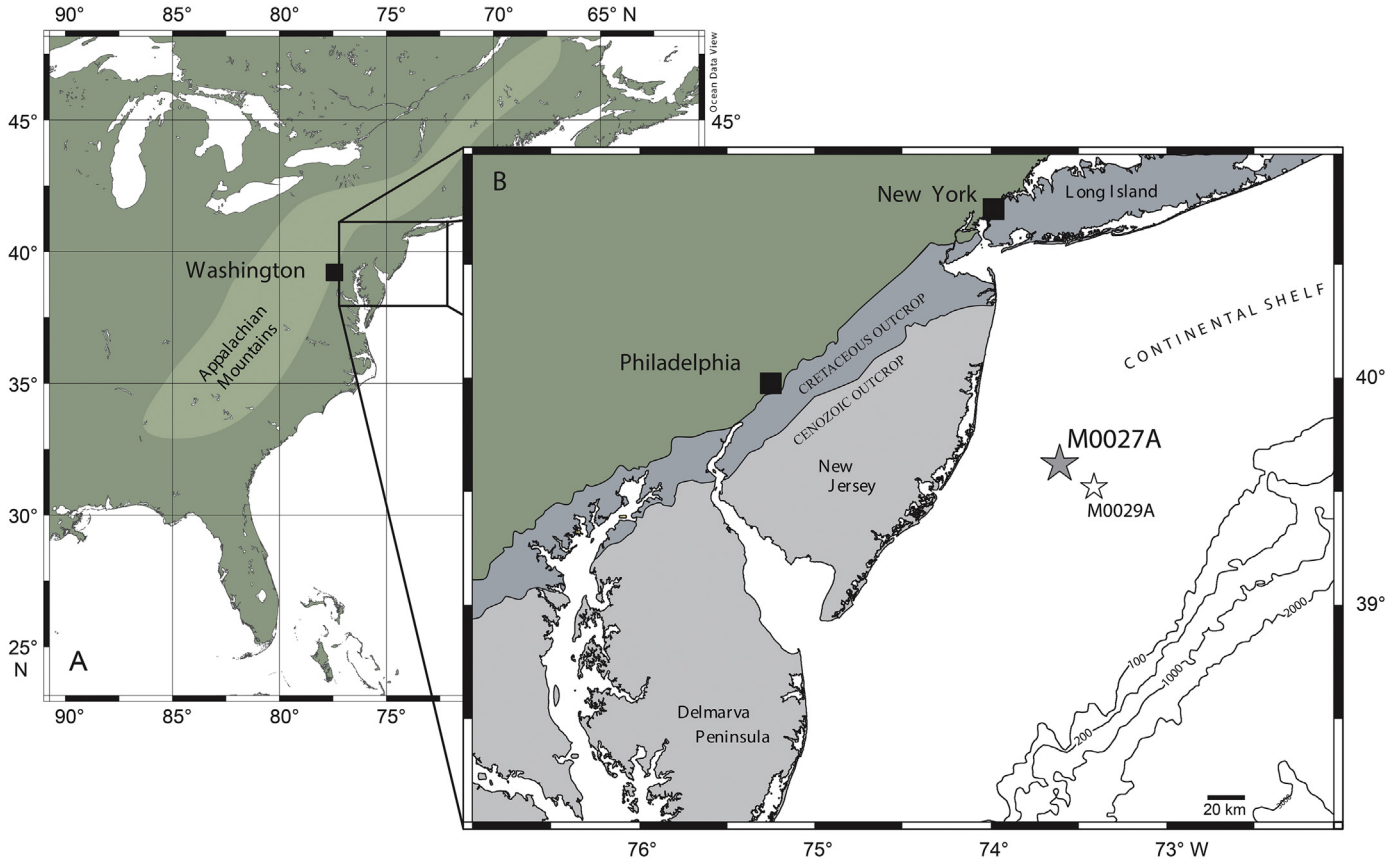

Fig. 1. A. Location of the study area in eastern North America. B. Detailed map of the New Jersey area. Gray star indicates position of Site M0027, white star: position of Site M0029. After Mountain et al. (2010), Schlitzer (2011), Kotthoff et al. (2014).

variation of the Appalachian Mountains started at ~20 Ma; prior to this time the Appalachians showed low relief and elevation (Liu, 2014).

2.2. Palynology

2.2.1. Sample processing and analyses

For the present study sample preparation was performed following a modified protocol of Bates et al. (1978) at Brock University, St. Catharines, Canada (sieving, HCl- and HF-treatment) and at the Laboratory of University of Hamburg (acetolysis). For all samples ~5 cm^3 sediment were disaggregated in 0.02% sodium hexamethaphosphate, treated with 25% hydrochloridic acid and subsequently with 48% hydrofluoric acid (HF) and sieved through a 10 μm Nitex mesh.

A small amount of the processed material was mounted in glycerine jelly. The remainder of the HF-treated material was subsequently acetolyzed following a modified protocol from Zetter and Ferguson (2001). Due to the moderate preservation, acetolyzation was performed without chlorination. In several samples, palynomorph preservation was limited so that further chemical treatment (acetolyzation) was completely omitted. In these cases, counting and identification of terrestrial palynomorphs were done using the material solely treated with HF.

Per sample, 300–400 terrestrial palynomorphs were identified using mostly the acetolyzed treated material. For percentage calculations, bisaccate pollen grains were excluded from the reference sum as these grains tend to be overrepresented in marine records (Mudie and McCarthy, 1994; Eldrett et al., 2009). Additionally, 300 marine/terrestrial palynomorphs were counted using the non-acetolyzed material due to sensitivity of gonyaulacoid (autotrophic) dinoflagellate cyst (dinocysts) and most of the thin-walled protoperidinoid dinocysts (heterotroph) to acetolysis (Mudie and McCarthy, 2006). The pollen versus dinoflagellate cyst ratio (P:D) acts as an indicator for transport mechanisms and sea level fluctuations (Mudie and McCarthy, 1994; McCarthy et al., 2013), where high P:D indicates low sea level and/or enhanced run off.

In sum, 56 samples were analyzed comprising several time intervals from the middle late Oligocene (Sequence O3 and Sequence O6) to the early Miocene (Sequence O6, Sequence m6 and Sequence m5.8). Sequence O3 includes 26 samples, 19 samples were counted for Sequence O6, and 10 for Sequence m6. An additional sample was counted for Sequence m5.8. Pollen grain identification and counting were done using a Zeiss Axioscope A1 at 630x magnification. Additionally, some pollen grains were analyzed via SEM using the single-grain technique (Hesse et al., 2009). We applied the Shannon-Wiener-Index (H(s)) in order to assess changes in diversity. The diagnosis of pollen grain ornamentation of different *Quercus* sections follows the descriptions of Grímsson et al. (2015) and Bouchal et al. (2014).

2.2.2. Taphonomy of terrestrial palynomorphs

Deposition of terrestrial palynomorphs in marine sediments depends on multiple factors (e.g., pollen production, transport mechanisms, shoreline distance; van der Kaars, 2001). Studies concerning deposition of pollen and spores in neritic marine sediments (Mudie and McCarthy, 1994; van der Kaars, 2001) indicate a reliable comparability of the microfloristic assemblage in marine sediments with the contemporary onshore vegetation. Because the paleoshelf break only transgressed the Site M0027 during the early Miocene (McCarthy et al., 2013, compare Fig. 2) dominance of bisaccate grains is expected, reflecting their preferential transport in wind and water (McCarthy et al., 2003).

In the present day the most important transport mechanism of pollen and spores into the marine realm along the North American coast are the westerlies (Mudie and McCarthy, 1994). Prevailing westerly

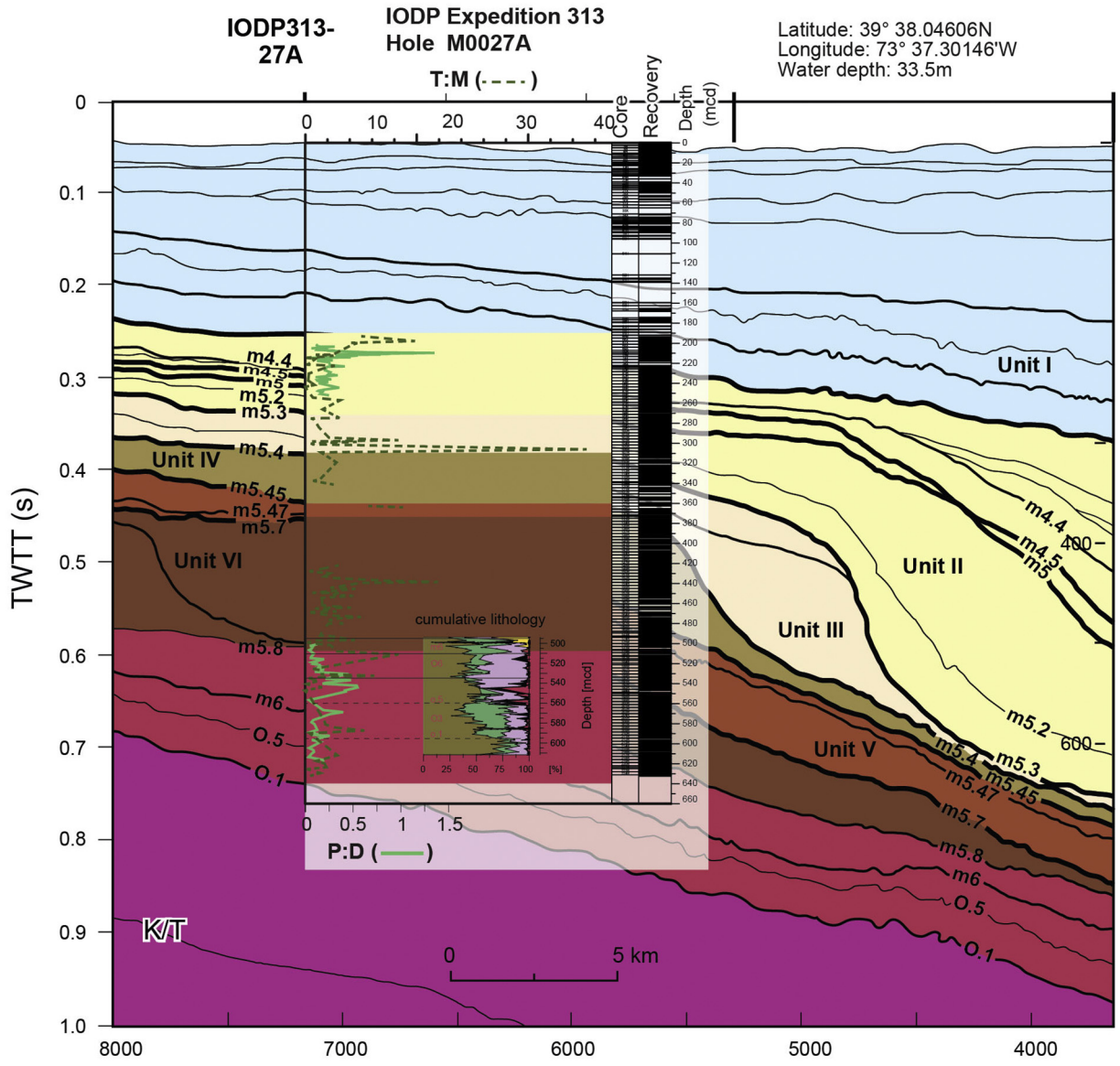

Fig. 2. Seismic profile through Site M0027 including T:M (terrestrial versus marine palynomorphs after McCarthy et al., 2013), P:D (pollen versus dinoflagellate cyst; this study: Oligocene to early Miocene; late Mid-Miocene after Prader et al., 2017) and cumulative lithology after Miller et al. (2013a). Rapid aggradation (vertical accumulation of sediment at times of sea level rise and high sedimentation rate) and progradation (displacement of coastline and clinoform) across the New Jersey margin is evident in the interpreted seismic record, particularly in the thick Unit VI/ Sequence m5.8. The P:D ratio reflects shifts in shoreline distance and major peaks in T:M record pulses of downslope mass wasting associated with glacioeustatic sea-level lowstands (McCarthy and Mudie, 1998). Mcd: meters composite depth corresponds with mbsf (meter below seafloor), K/T: Cretaceous–Tertiary boundary. Cumulative lithology: brown: clay and silt; green: glauconite; violet: fine quartz sand; yellow: medium and coarser quartz sand; black: carbonate; white: mica and other.

winds were probably already established by the middle Oligocene. A further, but subordinate transport mechanism is pollen input via rivers and streams into the NJSS. Fluvial influence has been identified based on the sedimentological record (Miller et al., 2013a) for the NJSS. Downslope mass transport is not expected to be a major factor at Site M0027 prior to the transgression of the shelf break within sedimentary Unit 6/sequence m5.8 (Fig. 2), except during glacioeustatic lowstands – then the ratio of terrestrial vs. marine palynomorphs ("P:D") helps identifying resedimentation (McCarthy et al., 2013; Donders et al., 2018).

2.2.3. Reconstruction of paleovegetation

Terrestrial palynomorphs were grouped into six generalized paleovegetation units: 1: high-altitude conifer forest; 2: mid-altitude conifer forest; 3: Cupressaceae; 4: mesophytic forest growing on well-drained soils; 5: mesophytic forest growing on moist/wet soils; 6: mesophytic understory; 7: plant community associated with coastal environments, growing on sun-exposed sandbanks. Numerous plant taxa are not restricted to a specific vegetation unit, but have tendencies to multiple and various habitat preferences (compare Table 1) making an unambiguous assignment difficult. The generalized grouping performed in this study allows inferring possible shifts within the terrestrial vegetation (e.g., Larsson et al., 2011).

Encountered bisaccate conifer pollen grains were assigned to mid- to higher altitude paleovegetation units farther further inland on the basis of the taphonomy of bisaccate grains. The only living species of *Cathaya*, *C. argyrophylla* thrives on ridges in mountainous regions together with evergreen broadleaf and deciduous taxa (Liu and Basinger, 2000) indicating an association of pollen grains derived from this taxon to the mesophytic forest growing on well drained soils. However, it is unclear how well the current distribution of *Cathaya* expresses the ancient ecological requirements of the taxon (Liu and Basinger, 2000). It probably thrived in the transition zone of the mesophytic forest and

Table 1
Summary of identified taxa for Site M0027 together with sources of climatic range and assignments to paleovegetation units, alphabetically ordered (bold: taxon assigned to a paleovegetation unit, other numbers: additional modern occurrence).

Taxon	Climate source	NLR used	Vegetation unit
Gymnosperms			
Abies	–		**1**
Cathaya	a	*C. argyrophylla*	**2**/4
Cupressaceae	–		1/2/**3**/4/5/6/7
Ephedra	–		1/2/**7**
Larix/*Pseudotsuga*	–		**1**
Picea	–		**1**
Pinus subg. *Pinus*	–		**2**/5/7
Pinus subg. *Strobus*	–		**2**/5/7
Sciadopitys	d	*S. verticillata*	**2**
Tsuga sp.1	b	*Tsuga* spp. (NA)	2/**4**/7
Tsuga sp.2	b	*Tsuga* spp. (NA)	2/**4**/7
Angiosperms			
Acer	b	*Acer* spp. (NA)	**4**/5
Alnus	–		1/2/**5**
Anacardiaceae	–		2/**4**/5
Apiaceae	–		4/**6**/7
Artemisia	–		1/2/**6**/7
Betula	–		2/4/**5**/7
Carpinus/*Ostrya*	b	*Carpinus* and *Ostrya* spp. (NA)	4
Carya	b	*Carya* spp. (NA)	2/4/**5**/7
Castaneoideae	b	*Castanea* spp./*Castanopsis chrysophylla*/ *Lithocarpus densiflorus*	2/**4**
Cedrelospermum?	–		?
Chenopodiaceae/Amaranthaceae	–		1/2/4/5/6/**7**
Clethra	–		4/**5**
Cornus	b	*Cornus* spp. (woody, NA)	1/2/**4**/5
Corylus	b	*Corylus* spp. (NA)	**4**/5
Cyperaceae	–		2/4/5/**6**
Diospyros	b	*Diospyros* spp. (NA)	**4**/5
Elaeagnus	–		2/**4**/5
Engelhardioideae	–		4
Ericaceae	–		1/2/**4**/5/6
Eucommia	a	*E. ulmoides*	**4**
Fabaceae	–		1/2/4/5/**6/7**
Fagus	b	*F. grandifolia*	**4**/2
Fraxinus	b	*Fraxinus* spp. (NA)	2/4/**5**
Gordonia	b	*G. lasianthus*	**5**
Hamamelidaceae	–		**4**/5/7
Humulus	–		4/**5**
Ilex	a	*Ilex* spp. (NA)	2/4/**5**
Itea	b	*I. virginica*	2/4/**5**
Juglans	b	*Juglans* spp. (NA)	4/**5**
Juglandaceae	–		**4**/5
Liliaceae	–		4/5/**6**/7
Liquidambar	b	*L. styraciflua*	**5**
Lonicera	–		2/**4**/5
Magnolia	b	*Magnolia* spp. (NA)	2/**4**/5/7
Myrica/*Morella*	a	*Morella* spp. (NA)	4/**5**/6
Nyssa	b	*Nyssa* spp. (NA)	4/**5**
Oleaceae	–		
Ostrya	b	*Ostrya* spp. (NA)	**4**
Parthenocissus	c	*Parthenocissus* spp. (NA)	**4**/5/7
Platanus	b	*Platanus* spp. (NA)	**4**/5
Poaceae	–		1/2/4/5/**6**
Prunus	b	*Prunus* spp. (NA)	2/**4**/5
Pterocarya	a	*Pterocarya* spp. (China)	1/**4**/5
Quercus	b	*Quercus* spp. (NA)	2/**4**/5/7
Reevesia	a	*Reevesia* spp. (China)	2/**4**/5
Rhamnaceae	–		4/**5**/7
Rosaceae	–		1/2/**4**/5/6/7
Salix	–		**5**
Sapotaceae	–		4/**5**
Symplocos	b	*S. tinctoria*	**5**
Tilia	b	*Tilia spp.* (NA)	**4**/5
Ulmus	b	*Ulmus spp.* (NA)	**5**
Ulmus/*Zelkova*	b	*Ulmus* spp. (NA)	**5**
Vitaceae	–		2/4/**5**
Vitis	–		2/4/**5**
Zelkova	a	*Zelkova* spp. (China)	**5**

(continued on next page)

Table 1 (*continued*)

Taxon	Climate source	NLR used	Vegetation unit
Pteridophytes			
Equisetum	–		1/2/4/**5**/6/7
Lycopodium	–		2/**5**/6
Osmunda	c	*Osmunda* s.l. (NA)	4/**5**/7
Polypodiaceae	–		1/2/**5**/6/7

1. high-altitude conifer forest; 2. mid-high-altitude conifer forest. 3. Cupressaceae 4. mesophytic forest growing on well-drained soils; 5. mesophytic forest growing on moist/wet soils; 6. mesophytic understorey; 7. plant community associated with coastal environments, growing on sun-exposed sandbanks. [a] Fang et al. (2011); [b] Fang et al. (2011); [c] Natural Resources Canada (2001); [d] GBIF (2001) + WorldClim (2005).

the mid-altitude conifer forest, although *Cathaya* could have also been part of swampy lowland environments. This interpretation is reinforced by findings of fossilized wood remains of *Cathaya* in Central Europe (Neogene) indicating to an adaptation to peat forming environments (Dolezych and Schneider, 2006, 2007, 2012).

According to this, pollen percentages of *Cathaya* were attributed to the mesophytic forest on moist to wet soils, forming the eighth paleovegetation unit. It probably flourished in swampy environments, most likely also together with various Cupressaceae taxa, which depend on higher soil water content. The assignment of bisaccate pollen grains to *Cathaya* (Plate I, 1) follows the specific morphological features mentioned in Grímsson and Zetter (2011).

2.2.4. Pollen grain identification, and paleoclimate

In this study, the bioclimatic analysis method after Greenwood et al. (2005) and Prebble et al. (2017) was used for paleoclimate reconstructions. Differences to the likewise NLR-based Coexistence Approach (Utescher et al., 2014) are described in detail in Prebble et al. (2017).

Pollen grains only identified at family level were generally excluded, since different representatives of a family can have considerable different growing preferences and would generate climatic overlaps of enormous range. The Juglandaceae subfamily Engelhardioideae, whose members have a very similar pollen grain ornamentation was also excluded, as well as several genera such as *Alnus* or *Betula*, since they presently flourish under heterogeneous macroclimatic conditions.

An unequivocal assignment of Cupressaceae pollen grains to genus level is problematic, and latest investigations recommend to avoid their allocation to genera (e.g., Grimm et al., 2015). According to this more conservative allocation, Cupressaceae pollen grains form the artificial paleovegetation unit 3. Cupressaceae grains were additionally subdivided into a papillate morpho-type and a non-papillate morpho-type (Plate I, 15–17). Similarly, encountered *Quercus* pollen grains were all assigned to the mesophytic forest growing on well drained soils, although in the extant North American oak species tolerate various edaphic conditions (Williams et al., 2006; eFloras, 2008).

In the case of the subfamily Castaneoideae (Fagaceae), which only rarely are distinguishable via scanning electron microscopy (Bouchal et al., 2014), we have generated a climatic envelope of the entire subfamily. The pollen ornamentation of the genera *Morella* and *Myrica* (Myricaceae) are identical (Grímsson et al., 2016b) and several former *Myrica* spp. are now included into the genus *Morella* (Herbert, 2005). The climatic profile used for our study is based on *Morella* spp. with exclusion of the boreal genus *Myrica gale* (compare Thompson et al., 2000a, 2000b, 2006). The genus *Craigia* (Tiloideae, Malvaceae), which was widespread during the Cenozoic in the Northern Hemisphere (Bůzek et al., 1989) but is today restricted to China and Vietnam (eFloras, 2008), has *Tilia*-like pollen grains (Kvaček et al., 2002). However, we used the climatic profile for *Tilia* in this case because the shape of the apertures and the tectum of the analyzed pollen grains of Site M0027 referred more to *Tilia* (Plate III, 15–16; Plate II, 8).

The generated paleoclimatic estimates: mean annual temperature (MAT), mean annual precipitation (MAP), and mean temperature of the coldest month (CMMT) and warmest month (WMMT) were based on climatic profiles taken from Thompson et al. (2000a, 2000b, 2006) for North American species and from Fang et al. (2011) for Chinese species. Additional plant taxon climate profiles are based on data from Natural Resources Canada (NRC, 2001) and the Global Biodiversity Information Facility (GBIF, 2001) using WorldClim (2005).

3. Results

3.1. Terrestrial palynomorphs

Fair preservation of pollen grains allowed for identification of 71 taxa. Table 1 gives a summary of all identified terrestrial palynomorphs. Light microscopy (LM) images of several well-preserved plant microfossils are shown on Plates I and II; Plate III illustrates SEM images of selected pollen grains.

Within the 56 analyzed samples, *Quercus* is the most abundant taxon with non-bisaccate pollen, represented probably by three sections: section *Quercus* (Plate III, 3–4), section *Quercus*/*Lobatae* (Plate III, 5–6), *Lobatae* (Plate III, 7–8) and aff. section *Protobalanus* (Plate III, 9–10). The number of *Quercus* pollen grains reaches >50% in most samples, except those at 572.15 and 570.02 mbsf (Fig. 3).

In addition, *Eotrigonobalanus* is also part of the microfloristic assemblage (Plate II, 20; Plate III, 11–12). Pollen grains with an *Eotrigonobalanus* affinity were counted 15 times (at 597.94, 584.73, 579.85, 570.02, 541.5, 535.46, 517.01, 513.01 mbsf). Pollen of the subfamily Engelhardioideae (Juglandaceae) is abundant too (min: 0.4%, max: 21.7%) and shows a decreasing trend toward Sequence m6 (20.9–20.7 Ma) (Fig. 3). Genera such as *Liquidambar*, *Elaeagnus* (Plate II, 3, 4) *Acer* (Plate I, 21), *Fagus*, *Nyssa* and *Artemisia* (Plate II, 12, 13) are sporadically present as are spores of pteridophytes.

The most abundant pollen grains of gymnosperms are those of *Pinus* (0.4% to 32.7%) and *Cathaya* (0% to 27.1%; Plate I, 1). Pollen grains of *Pinus* subg. *Strobus* outnumbered *Pinus* subg. *Pinus* in all samples (Fig. 3). The subdivision of *Pinus* at subgeneric level and of bisaccate pollen in general was often hindered by limited preservation. The sum of bisaccate representatives fluctuated through the entire analyzed time interval and reached the highest relative abundance of 120.8% (with bisaccate pollen excluded from reference sum) at 533.45 mbsf (Fig. 3). Relative abundances of *Pinus* and *Cathaya* (Fig. 3) have peaks at 597.94 mbsf (Fig. 3) and repeated peaks also occurred between 580 and 560 mbsf. During the same time interval, increased relative amounts of *Picea* (e.g., 6.3% at 572.15 mbsf) and *Abies* (1.0% at 574.04 mbsf) coincide with increased occurrence of *Larix*/*Pseudotsuga* pollen grains (Plate I, 6; Fig. 3). All these taxa are assigned to the high-altitude conifer forest.

The relative abundances of pollen grains of the family Cupressaceae fluctuate as well, of which pollen grains of the papillate morpho-type (Plate I, 12) are most abundant. Their relative abundance through the

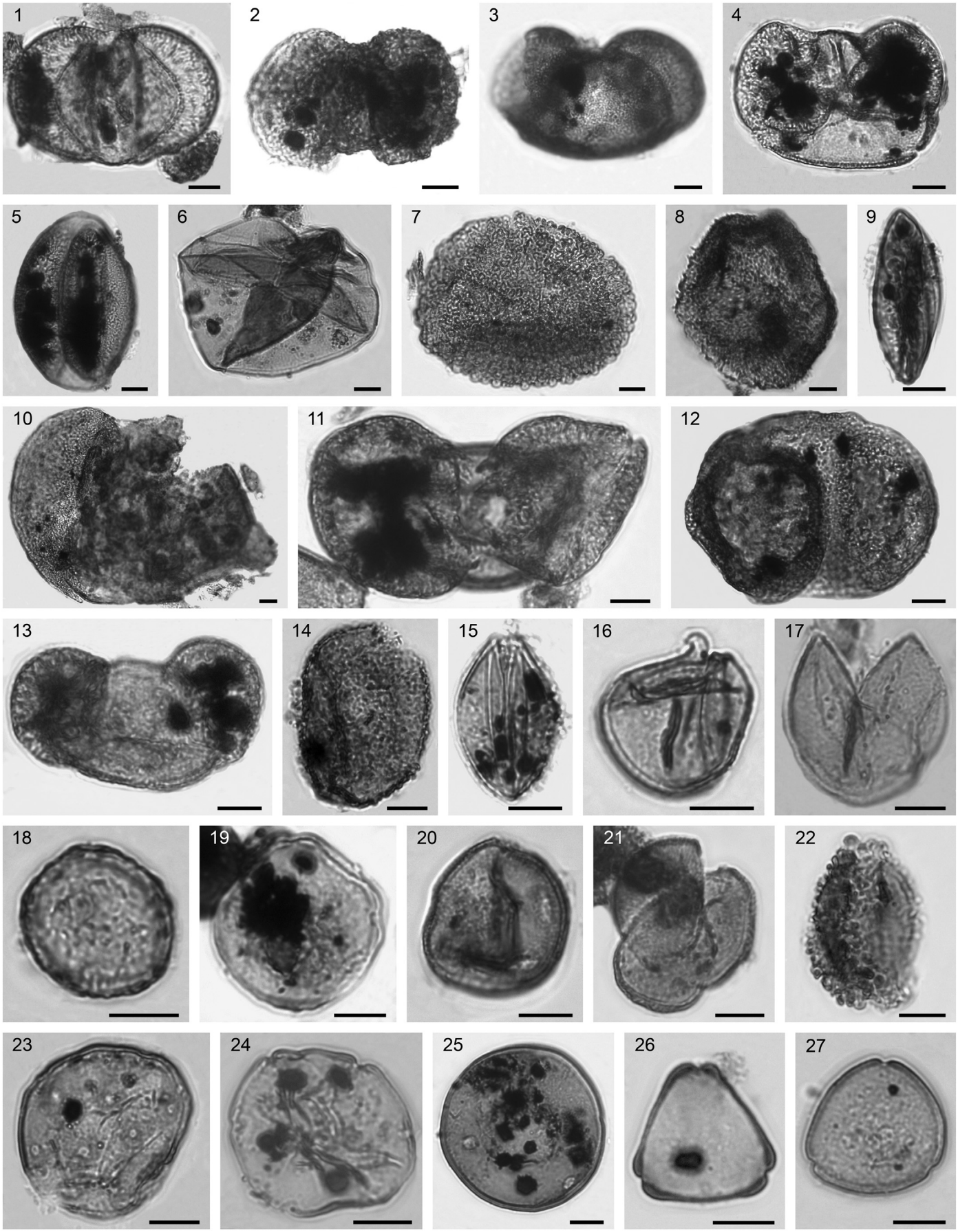

Plate I. LM images of selected pollen grains of identified taxa of Site M0027 (scale bar = 10 μm). 1. *Cathaya* (535.46 mbsf), 2. *Cathaya* (537.38 mbsf), 3. Pinaceae (518.03 mbsf), 4. *Picea* sp.1 (562 mbsf), 5. *Picea* sp.2 (495.91 mbsf), 6. *Larix*/*Pseudotsuga* (495.91 mbsf), 7. *Tsuga* sp. 1 (570.02 mbsf), 8. *Tsuga* sp. 2 (574.05 mbsf), 9. *Ephedra* (582.02 mbsf), 10. *Abies* (579.85 mbsf), 11. *Pinus* subg. *Pinus* (560.01 mbsf), 12. *Pinus* subg. *Strobus* (584.92 mbsf), 13. *Pinus* subg. *Strobus* (584.92 mbsf), 14. *Sciadopitys* (495.91 mbsf), 15. Cupressaceae non-papillate (541.5 mbsf), 16. Cupressaceae papillate (495.32 mbsf), 17. Cupressaceae presumably with papilla (541.5 mbsf), 18. *Ulmus* (498.54 mbsf), 19. *Zelkova* (560.01 mbsf), 20. *Liquidambar* (574.05 mbsf), 21. *Acer* (601.88 mbsf), 22. *Ilex* (601.88 mbsf), 23. *Juglans* (495.91 mbsf), 24. *Pterocarya* (495.72 mbsf), 25. *Carya* (540.3 mbsf), 26. Engelhardioideae (540.3 mbsf), 27. Engelhardioideae (533.54 mbsf).

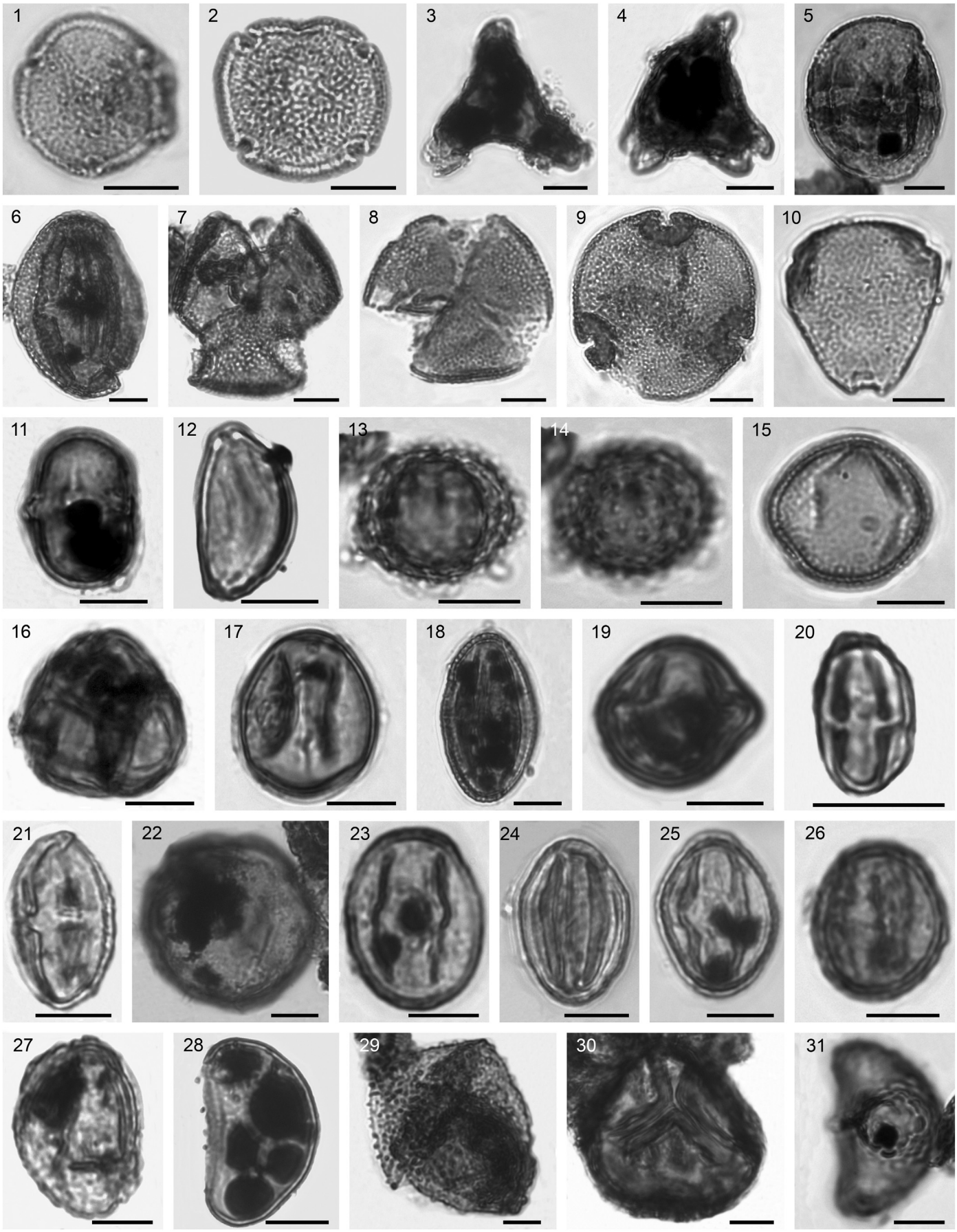

Plate II. LM images of selected pollen grains of identified taxa of Site M0027A (scale bar = 10 μm). 1. *Reevesia* (591.98 mbsf), 2. *Reevesia* (603.58 mbsf), 3. *Elaeagnus* (601.88 mbsf), 4. *Elaeagnus* (597.94 mbsf), 5. Sapotaceae (597.94 mbsf), 6. *Gordonia* (600.16 mbsf), 7. *Gordonia* (509 mbsf), 8. *Gordonia* same pollen grain as in Plate I (574.05 mbsf), 9. *Tilia* (597.94 mbsf), 10. *Symplocos* (570.02 mbsf), 11. Fabaceae (579.85 mbsf), 12. *Itea* (584.92 mbsf), 13. *Artemisia*: middle view (521.62 mbsf), 14. *Artemisia*: upper view (521.62 mbsf), 15. *Fraxinus* (611.76 mbsf), 16. Ericaceae (520.9 mbsf), 17. *Eucommia* (521.62 mbsf), 18. *Parthenocissus* (495.91 mbsf), 19. *Clethra* (574.05 mbsf), 20. Castaneoideae (494.91 mbsf), 21. *Eotrigonobalanus*; same pollen grain as in Plate III (574.05 mbsf), 22. *Fagus*; same pollen grain as in Plate III (574.05 mbsf), 23. *Quercus* section *Quercus*/*Lobatae*; same pollen grain as in Plate III, 5–6 (574.05 mbsf), 24. *Quercus* section aff. *Protobalanus*; same pollen grain as in Plate III, 9–10 (574.05 mbsf), 25. *Quercus* section *Quercus* same pollen grain as in Plate III, 3–4 (574.05 mbsf), 26. *Quercus* (574.05 mbsf), 27. *Quercus* (585.7 mbsf), 28. Polypodiaceae (584.73 mbsf), 29. *Osmunda* (574.05 mbsf), 30. Trilete spore indet. (509 mbsf), 31. Spore indet. (532.62 mbsf).

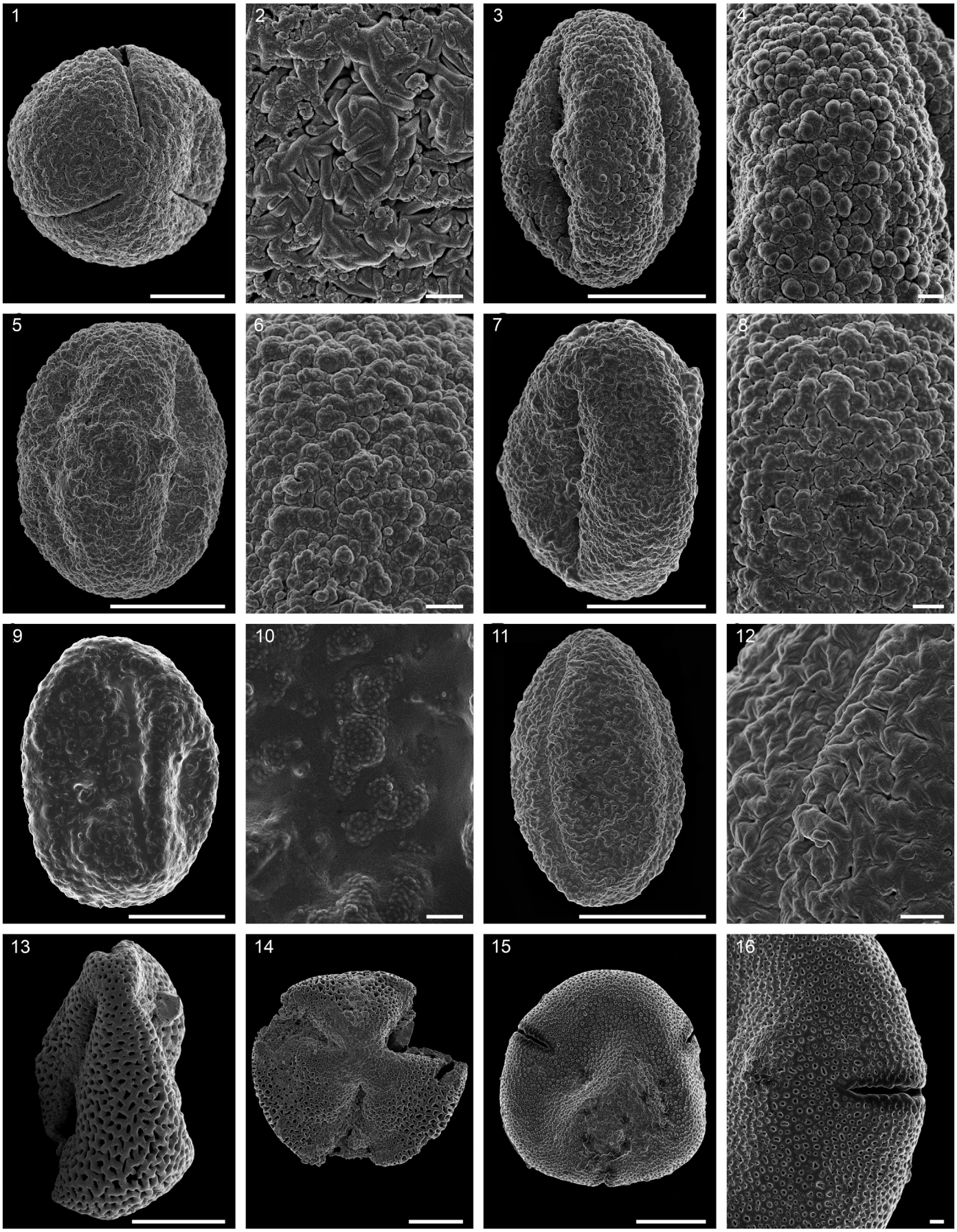

Plate III. SEM images of selected pollen grains of Site M0027A (574.05 mbsf). Overview (1, 3, 5, 7, 9, 11, 13, 14, 15) and detail (2, 4, 6, 8, 10, 12, 16). 1–2: *Fagus*; 3–4: *Quercus* section *Quercus*; 5–6: *Quercus* section *Quercus/Lobatae*; 7–8: *Quercus* section *Lobatae*; 9–10: *Quercus* aff. section *Protobalanus*; 11–12: *Eotrigonobalanus*; 13–14: *Gordonia*; 15–16: *Tilia*. Scale bar 10 μm (1, 3, 5, 7, 9, 11, 13, 14, 15), 1 μm (2, 4, 6, 8, 10, 12, 16).

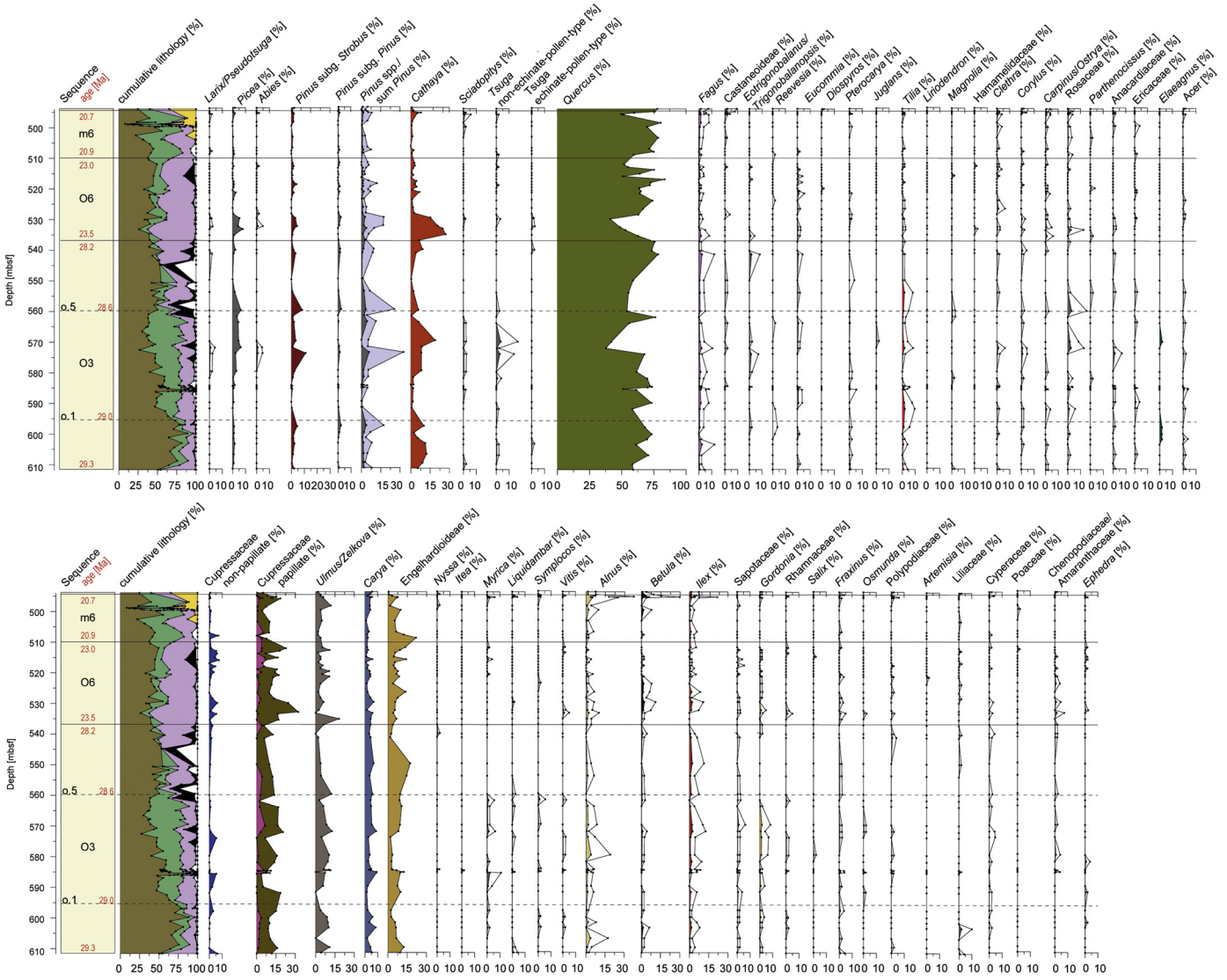

Fig. 3. Relative abundances (percentages) of pollen grain taxa for Site M0027A plotted against depth (pollen sum excluding bisaccates). Transparent areas all in plots denote 5x exaggerated values. *Pinus* ssp.: gray, sum of encountered *Pinus* pollen grains including destroyed pollen grains: yellow. Cupressaceae presumably with papilla: pink; Cupressaceae with a papilla: brown. Sequence boundaries and age model after Browning et al. (2013) and Miller et al. (2013a, 2013b) with dashed lines indicating sequence boundaries. Cumulative lithology after Miller et al. (2013a): brown: clay and silt; green: glauconite; violet: quartz sand; yellow: medium and coarser quartz sand; black: carbonate; white: mica and other.

analyzed time interval shows distinct peaks at around 29.0 Ma (591.98 mbsf with 18.5%) and between 580 and 560 mbsf. A marked count of Cupressaceae pollen grains occurred again at the beginning of Sequence O6 (Figs. 3 and 4). The abundance of pollen grains assigned to mesophytic forest on moist/wet soils slightly varies through the analyzed time interval and shows a similar fluctuations behavior as the Cupressaceae.

The mesophytic forest growing on dry soils is characterized by deciduous broadleaf taxa such as *Quercus*, *Tilia*, *Eucommia*, *Fagus*, and *Reevesia* (Plate II, 1 and 2), and furthermore by *Magnolia* (Table 1; Fig. 3). Through the analyzed time interval, the relative contribution of this paleovegetation unit shows an average value of 73.9%. However, at 572.15 mbsf (Sequence O3; ~29.3 to ~28.2 Ma) and at 529.97 mbsf (Sequence O6; ~23.5 to ~23.0 Ma) it lost ~20% of its average amount (Fig. 4).

The pollen dinoflagellate cyst ratio (P:D) is highest at the end of Sequence O3 and at the beginning of Sequence O6 (Fig. 4). The Shannon-Wiener Index (H(s)), generally varies between 1 and 2 indicating relatively low diversity, but shows distinct peaks >2 between 560.01 and 572.15 mbsf, 529.97 and 533.54 mbsf, and 495.72 and 495.91 mbsf, respectively (Fig. 4).

3.2. Estimated paleoclimate of NJSS

The bioclimatic analysis indicates humid warm-temperate climatic conditions for the entire dataset (Fig. 5). Average estimated MAT for the entire record was 14.6 °C ± 4.0 °C. Paleoclimatic estimates of CMMT are 5.2 °C ± 5.3 °C and of WMMT 24.1 °C ± 2.9 °C on average. All average paleoclimatic estimations for each individual sequence are summarized in Table 2. The paleoclimatic conditions of the New Jersey hinterland remained relatively constant over the preserved interval, with long-term MAT change limited to 2–3 °C.

Considering each investigated sequence individually, an average weak cooling and warming is reflected within the humid warm-temperate climate (compare Table 2). Around the OMB (Fig. 5) between ~533 and ~529 mbsf a stepwise decline to lower temperatures is reflected (MAT and WMMT ~-3 °C; CMMT ~-5 °C). The only estimated paleoclimatic parameter which remained fairly constant over the

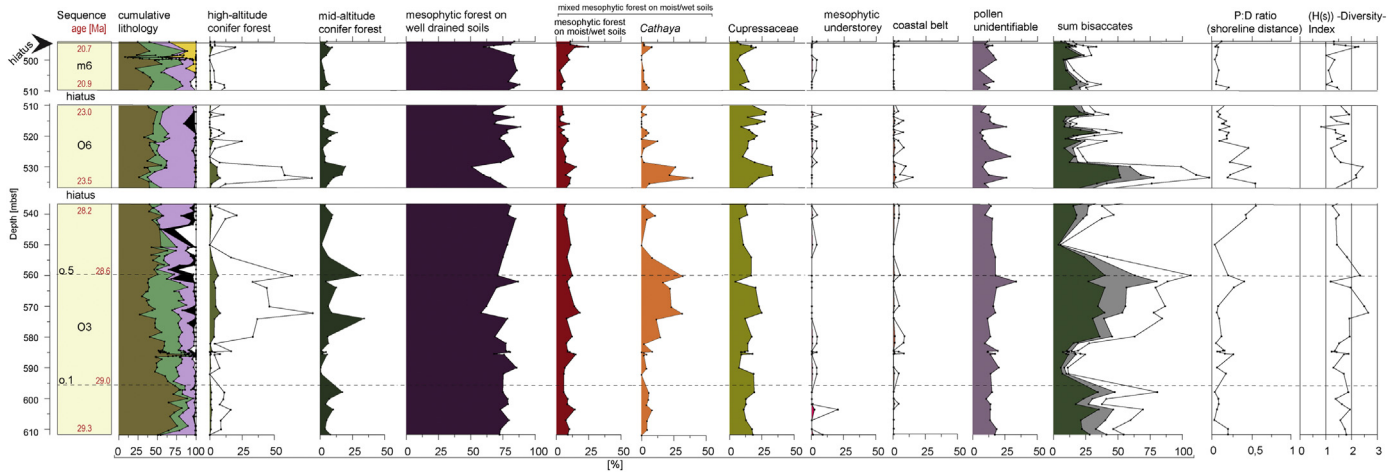

Fig. 4. Relative abundances (percentages) of paleovegetation units of the NJSS hinterland during the middle Oligocene to early Miocene as well as the H(s))-diversity-index and the pollen-dinoflagellate ratio (P:D) indicating site-shoreline distance plotted against depth. Taxa are assigned as listed in Table 1 (transparent: 10x exaggerated: high-altitude conifer forest; mesophytic understorey and coastal belt); sum of bisaccates: gray: unassigned bisaccate pollen grains; green: percentages of destroyed parts of bisaccate pollen grains. Sequence boundaries and age model after Browning et al. (2013) and Miller et al. (2013a, 2013b): dashed lines: sequence boundaries. Cumulative lithology after Miller et al. (2013a): brown: clay and silt; green: glauconite; violet: quartz sand; yellow: medium and coarser quartz sand; black: carbonate; white: mica and other.

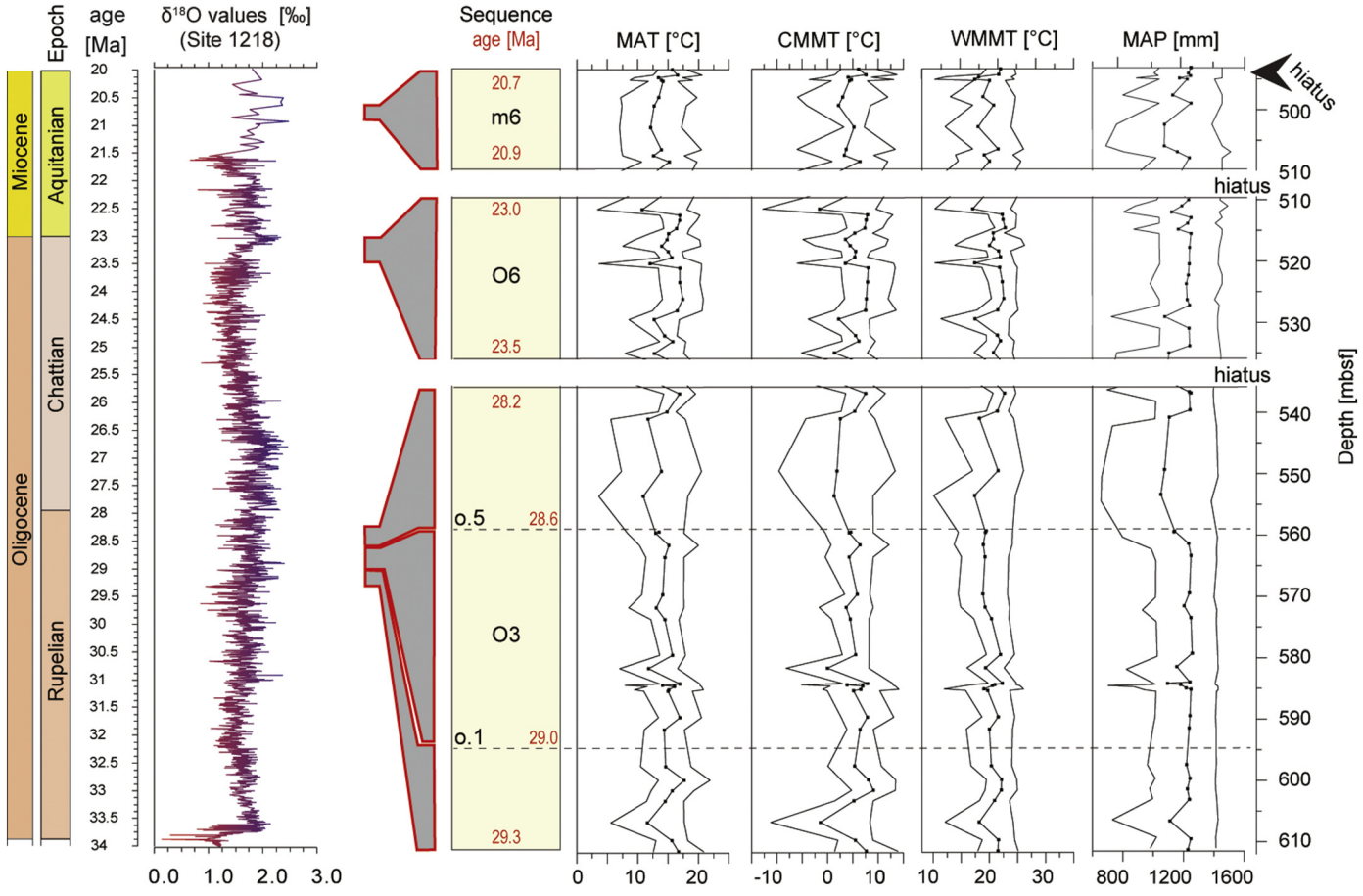

Fig. 5. Calculated paleoclimate during the middle Oligocene and early Miocene for the hinterland of the NJSS based on identified pollen grains from Site M0027 following the bioclimatic analysis after Greenwood et al. (2005) and Prebble et al. (2017) plotted against depth. Compared with $\delta^{18}O$ values of ODP Site 1218 (equatorial Pacific) after Wade and Pälike (2004) plotted against age. Consider the different age models. Red: warmer time intervals, blue: cooler time intervals. MAT: mean annual temperature; CMMT: coldest moth mean temperature; WMMT: warmest month mean temperature and MAP: mean annual precipitation; outer lines: error of estimated values (present day climate parameters of Toms River (New Jersey): MAT 11.7 °C; CMMT: 5.7 °C; WMMT: 17.7 °C; MAP: 1239 mm, after US Climate Data, 2017).

Table 2
Summary of average climatic values and average errors of estimated values for each analyzed sequence from the middle and late Oligocene and early Miocene (Sequence m5.8 compromises only one analyzed sample).

Sequence	MAT [°C]	CMMT [°C]	WMMT [°C]	MAP [mm]
O3	14.0 (±4.1)	4.1 (±5.1)	23.9 (±3.0)	1312.2 (±293.9)
O6	15.0 (±3.6)	5.5 (±5.2)	24.5 (±2.4)	1332.6 (±278.8)
m6	13.8 (±4.8)	4.4. (±6.0)	23.5 (±3.6)	1297.4(±324.2)
m5.8	15.4 (±2.5)	6.1 (±4.0)	24.8 (±1.9)	1359.9 (±270.1)

analyzed time is MAP (Table 2; Fig. 5), reflecting humid conditions (always >1000 mm).

4. Discussion

4.1. Paleoforests of New Jersey's hinterland in a regional context

Our results indicate that the Oligocene hinterland of the NJSS was covered by dense forests, with mesophytic forest growing on well-drained soils being the most widespread and diverse forest type on areas of low relief. The younger and more northerly megaflora of the Brandon Lignite, Vermont (early middle Miocene: e.g., Tiffney, 1977, 1979; Tiffney and Barghoorn, 1979; Tiffney, 1993, 1994; Tiffney et al., 2018) includes seeds, fruits and wood remains, and is interpreted as a local forest community dominated by angiosperm trees (Tiffney, 1994). This local flora, however, had a more broadleaf evergreen character (Tiffney, 1994) than the palynoflora from the New Jersey hinterland. The Brandon Lignite megaflora contains fruits and seed remains of *Persea* and other Lauraceae, *Zanthoxylum* (Rutaceae), *Illicium* (Schisandraceae) and *Symplocos* (Symplocaceae) (Tiffney, 1993; Tiffney, 1994; Tiffney et al., 2018). However, the fossilization potential of Lauraceae pollen grains is generally low (Herendeen et al., 1994) due to their particularly thin sporopollenin-containing exine. This preservation bias explains the lack of such pollen in the New Jersey shelf sediments as well as in the palynoflora of the Brandon Lignite (Traverse, 1994). Higher elevations of the New Jersey hinterland, and/or drier areas were probably inhabited by conifers such as Pinaceae. The pollen assemblage of the Brandon Lignite contains various bisaccate pollen of different form-genera referred to *Picea*, *Pinus* and probably *Cathaya* (Traverse, 1994). However, findings of conifer megafossils are not mentioned (e.g., Tiffney, 1977, 1979; Tiffney and Barghoorn, 1979; Tiffney, 1993, 1994), implying that conifers were restricted to small suitable areas of the regional catchment area. *Abies* or *Tsuga* pollen grains are not reported from the palynoflora of the Brandon Lignite (Traverse, 1994), while two different pollen morpho-types of *Tsuga* (Plate II, 7–8) were found in the core sediments of New Jersey (i.e., NJSS).

The close similarity of the New Jersey and the Brandon Lignite palynofloras is shown by the share of a substantial number of plant genera such as *Itea* (Plate II, 11), *Parthenocissus* (Plate II, 17) or *Gordonia* (Plate II, 6–8) and other plant genera commonly distributed in the Northern hemisphere during the Cenozoic, such as *Pterocarya*, *Ilex*, *Liquidambar*, *Symplocos* or Sapotaceae (Table 1 for the New Jersey Shelf; Traverse (1994) for Brandon Lignite). The scarcity of herbaceous taxa in both areas indicates that during the Oligocene and early Miocene open landscapes were rare in north-eastern North America. Oak (*Quercus* spp.) pollen grains were the dominant and characteristic palynofloristic element of both the Brandon Lignite (Traverse, 1955 sine Tiffney, 1993) and the New Jersey hinterland.

4.2. Paleofloristic composition with special reference to the genus Quercus

Oaks dominated the mesophytic forest of eastern North America in the past and still do in the present day (Abrams, 1992). In the present day ~90 different *Quercus* species are found in North America, of which ~35 species are present in eastern North America (eFloras, 2008). Modern oak lineages became established during the early Paleogene (Barrón et al., 2017), for which the first unequivocal fossil evidence in North America is from Oregon (late early Eocene; Manchester, 1994, 2011). A palynofloristic record from southern Mississippi and Alabama (Oboh and Reeves Morris, 1994; Oboh et al., 1996) revealed that oaks became dominant around the Eocene–Oligocene boundary in south-eastern North America. The vegetation shift was potentially triggered by cooling and drying, as suggested by Frederiksen (1980, 1991). However, it is unclear how many of the encountered *Quercoidites* are solely related to the genus *Quercus* Frederiksen (1980, 1991).

The currently accepted classification of *Quercus* supports the division of the genus in two subgenera (subgenus *Quercus* and *Cerris*) with eight sections (Denk et al., 2017 and references therein). According to this classification, the fossil record of oaks in North America was highly diverse, comprising species of both subgenera (Denk et al., 2017) with four sections (Denk et al., 2010 and references therein), of which subgenus *Cerris* was represented by section *Cyclobalanopsis* (Bouchal et al., 2014). In the modern North American vegetation, however, only subgenus *Quercus* persists with five sections, of which sections *Lobatae* (red oaks), *Quercus* (white oaks) and *Virentes* (live oaks) exist east of the Cordillera (Denk et al., 2017). The different sculptures of oak pollen grains within sections of both subgenera generally vary from rugulate, e.g., in section *Ilex*, through verrucate, e.g., in section *Cerris*, to weakly verrucate, perforate in section *Protobalanus* (Denk et al., 2017 and references therein). Considering the analyzed *Quercus* pollen grains from our study, the pollen grain sculptures represent subgenus *Quercus*, including most likely section *Quercus* (Plate III, 3–4) *Quercus*/*Lobatae* (Plate III, 5–6), *Lobatae* (Plate III, 7–8) and aff. Section *Protobalanus* (golden-cup oaks; Plate III, 9–10).

Today *Quercus* section *Protobalanus* is restricted to western North America (eFloras, 2008). Pollen grains with similar ornamentation morphology are described from sediments of western Greenland (middle Eocene; Grímsson et al., 2015). However, the pollen ornamentation of section *Protobalanus* could possibly also indicate an ancestral lineage of the Protobalanus–Quercus–Lobatae clade (Grímsson et al., 2015). Several pollen grains assigned to section *Quercus* could however, also belong to section *Virentes*. Pollen grain analyses of modern *Q. virginiana* (section *Virentes*; former section *Quercus*) show similarities in their sculpturing to members of section *Quercus* (Denk and Grimm, 2009). Phylogenetic age estimations of section *Virentes* suggest a split from its sister section *Quercus* of ~11.0 Ma and a speciation event within section *Virentes* at ~5.0 Ma (Cavender-Bares et al., 2015). If this was correct, no representatives of section *Virentes* could have grown in the New Jersey hinterland during the analyzed time interval and pollen grains with this typical sculpturing can be considered as pollen grains of representatives of section *Quercus*. A more recent study implies a phylogenetic split of Section *Virentes* from section *Quercus* around the OMB (Hipp et al., 2019). Following this phylogenetic analysis representatives of Section *Virentes* might have also been part of the hinterland vegetation producing a share of deposited pollen grains in core sediments of New Jersey. However, these interpretations are speculative since different phylogenetic studies can have highly different outcomes of crown age estimates (Willis and McElwain, 2014). Due to the lack of unambiguous macrofossil evidence of *Quercus* section *Virentes* (Cavender-Bares et al., 2015; Denk et al., 2017) to support this interpretation, no clear conclusion can be made in this case confirming the growth of section *Virentes* in the New Jersey hinterland during the Oligocene and early Miocene. Today the entire section is restricted to lower elevations of North and Central America (Cavender-Bares et al., 2004), thriving under temperate conditions with mild winters and/or seasonal drier phases (Cavender-Bares et al., 2011).

The most frequently encountered pollen grain ornamentation in our investigation belongs to species from section *Lobatae*, which at present dominate in eastern North America (eFloras, 2008). Our data indicate

that the section *Lobatae* has remained the most important phylogenetic oak lineage in eastern North America since the Oligocene.

The NJSS microfloristic assemblages also suggest the presence of *Eotrigonobalanus* (Plate III, 11–12; Fig. 3), an extinct Fagaceae lineage. *Eotrigonobalanus* was a typical member of evergreen forests of the Paleogene and flourished in different ecological habitats (Walther, 2000). In Europe, *Eotrigonobalanus* was an accessory element within the evergreen forest during the middle Eocene (Walther, 2000), and became dominant during the late Eocene (Walther, 2000). In light of this, *Eotrigonobalanus* was probably an accessory element and scattered across the New Jersey hinterland during the Oligocene and early Miocene rather than a dominant tree as reported from Greece were *Eotrigonobalanus* was one of the prevalent forest elements during the late Oligocene (Velitzelos et al., 1999). This is most likely reflected by the sporadically encountered pollen grains through the analyzed time interval (compare Section 3.1).

There is evidence for the existence of *Triogobalanopsis*, another extinct Fagaceae lineage in North America, which is known from British Columbia, Canada (Eocene; Grímsson et al., 2016). Our SEM investigations revealed that all analyzed pollen grains in our study belong to *Eotrigonobalanus*, not *Triogobalanopsis*. However, we cannot rule out that *Triogobalanopsis* also flourished in the New Jersey hinterland. Both pollen grains look fairly similar under the light microscope and have been classified in the past under the form-genus *Tricolporopollenites cingulum* (Potonié, 1931) or *Tricolporopollenites cingulum* subsp. *fusus* (Thomson and Pflug, 1953), including as well other castaneoid-like genera (Walther and Zetter, 1993).

All analyzed *Eotrigonobalanus* pollen grains in this study comprise a lalongate endoaperture (Fig. 2, 20), which is considered to be a characteristic morphological structure for *Eotrigonobalanus* (Hofmann and Gregor, 2018).

Beside this similarity *Eotrigonobalanus* pollen of this study demonstrates additionally the pollen ornamentation characteristic of *Eotrigonobalanus eiszmannii* (Walther and Zetter, 1993) and of *Eotrigonobalanus* pollen grains found in British Columbia (Eocene) and Wyoming (Cretaceous; Grímsson et al., 2016).

The fossil record of *Eotrigonobalanus* in North America is very fragmentary (Grímsson et al., 2016) and this taxon is not reported from Brandon Lignite in Vermont (middle early Miocene; Traverse, 1994). In situ pollen grains from Texas referred to *Amentoplexipollenites* (late Rupelian to Chattian; Crepet and Nixon, 1989) have a very similar pollen ornamentation to those of our investigation as well as to *Eotrigonobalanus* pollen grains of Central Europe (Denk et al., 2012). However the lack of light microscopical images of *Amentoplexipollenites* (Crepet and Nixon, 1989) as stated by Hofmann and Gregor (2018) inhibits the endoaperture comparison. After Grímsson et al., 2016, a main characteristic difference between *Amentoplexipollenites* (Crepet and Nixon, 1989) and pollen grains of *Eotrigonobalanus* from British Columbia (Eocene) and Wyoming (Cretaceous) is the much thinner nexine of the latter. SEM investigations showed that the sculpturing of *Eotrigonobalanus* can be highly variable (compare Hofmann and Gregor, 2018).

4.3. Relative abundances of taxa of New Jersey's hinterland from the middle Oligocene to the late Miocene

Oaks remained relatively common floristic elements within the mesophytic forest during the Oligocene relative to the late Mid-Miocene (Prader et al., 2017); however, significant floristic shifts within the mesophytic forest occurred. Relative abundances of pollen grains of Engelhardioideae and *Carya* at New Jersey reveal similar values as at the eastern coast of the Gulf of Mexico and South Carolina for the late Eocene/early Oligocene (Frederiksen, 1991; Oboh and Reeves Morris, 1994; Oboh et al., 1996).

The Engelhardioideae (Juglandaceae) might have had a wider ecological range in the Oligocene–Miocene than reflected by their living representatives (Kvaček, 2007). However, the decreasing relative abundance of Engelhardioideae pollen in the long-term trend from the middle Oligocene to the late Miocene reveals that this group was not as competitive as other taxa facing environmental changes. Accordingly, this group is not prominent any more in the pollen record of the late Mid-Miocene (Prader et al., 2017). If this decrease was temperature-dependent, subsequent cooling events after the Mi-1 inception probably caused the disappearance of the taxon (Prader et al., 2017).

In comparison, other tree taxa such as *Fagus* or *Liquidambar* were more constant elements of the mesophytic forest during the Miocene (Prader et al., 2017) than during the Oligocene. The fossil records of *Fagus* (Denk and Grimm, 2009b) and *Liquidambar* (Manchester, 1999) for the Oligocene are fragmentary. These genera were also not prevalent in the New Jersey hinterland during the analyzed time interval.

Fagus appeared the first time in the fossil record during the early Paleocene (Danian) in western Greenland (Grímsson et al., 2016b) and was continuously widespread during the late Oligocene in the western part of the continent and Europe (Kvaček and Walther, 1991). Its radiation and diversification led to a first occurrence peak in the Miocene (Denk and Grimm, 2009b). Our investigations indicate that *Fagus* was only a minor vegetation element in the hinterland of the NJSS during the Oligocene, but relative abundances increased and *Fagus* became one of the dominant floristic elements toward the Mid-Miocene (Prader et al., 2017), indicating expanded habitats for *Fagus* and its radiation.

The analyzed pollen grains in this study have very long colpi (Plate III, 1–2), which is a typical pollen morphological feature of modern Asian species of *Fagus* subg. *Engleriana* and *F. grandifolia* (Denk, 2003). The modern species *F. grandifolia* (subg. *Fagus*) is native to eastern North America and closely related to subgenus *Engleriana* as inferred by phylogenetic analysis and morphology (Denk et al., 2005). Biogeographical reconstructions suggest that their ancestral lineages probably diverged from a common western North American *Fagus* population (Denk et al., 2005).

Contrary to the situation for *Fagus grandifolia*, which is the only native beech species in North America (eFloras, 2008), the Atlantic east coast is currently a biodiversity hot spot of the genus *Carya* (Wen, 1999). In our record, the relative occurrences of this genus were as low as those of *Fagus*. *Carya* first appeared in the Paleocene in North America (Manchester, 1987) and the first radiation began in the early Miocene (Zhang et al., 2013). Zhang et al. (2013) suggest that the Appalachian uplift phases created new habitats, which led to a diversification of the genus. This might explain the increase of the pollen grain counts of *Carya* in the Mid-Miocene where *Carya* became the dominant genus of the Juglandaceae in the New Jersey hinterland (Prader et al., 2017).

4.4. Long-term terrestrial ecosystem responses to middle Oligocene to early Miocene glacial events

4.4.1. Time correlation of Oligocene/early Miocene glacial events at the New Jersey margin

The entire Oligocene epoch is characterized by periodic climate oscillations associated with orbital insolation changes (Pälike et al., 2006). These orbital climate changes triggered the build-up and decay of Antarctic Ice Sheets, leading to substantial glacioeustatic sea level oscillations (Pekar et al., 2002, 2006; Wade and Pälike, 2004; Pälike et al., 2006). The hiatuses recognized in our record probably correspond to glacioeustatic low-stands during significant cooling events (Browning et al., 2013; Miller et al., 2013a). But even if our record may not reveal the maxima of such events, their onsets and offsets and minor cooling phases might be reflected, as well as the long-term post-glacial developments.

Such cooling signals within pollen-based climate reconstructions for the New Jersey hinterland are indicated by short MAT oscillations of max. 3–4 °C (e.g. at ~510 mbsf; Fig. 5). In addition to the possibility that our record misses cooling maxima due to interrupted

sedimentation, this limited variation might also be associated with the distinct marine influence, which buffered the regional impact of global climate changes in the hinterland. Furthermore, since the bioclimatic analyses technique is based on absence/presence of taxa, it is also possible that smaller climate signals are only reflected as abundance shifts.

Reconstructions of bottom water temperatures in the equatorial Pacific (Mg/Ca temperature records of Site 1218) indicate low temperature variations for the entire Oligocene (on average 3.7 ± 1.5 °C; Lear et al., 2004). However, rapid cooling of 2 °C is associated with isotope events Oi-2b and Mi-1 (Lear et al., 2004; Mawbey and Lear, 2013). The Oi-2a cooling event at 28.3 Ma (Pekar and Miller, 1996; Pekar et al., 2002) as well as the Oi-2b event which took place around 27.1 Ma (Pekar et al., 2002) are linked to glacioeustatic low-stands which created the large hiatus between Sequence O3 and O6 at the NJSS (Browning et al., 2013; Miller et al., 2013a). The age model of Pekar et al. (2002) for the New Jersey margin indicates that the Oi-2a cooling event should be represented in our record, but it is not completely congruent with the age model by Browning et al. (2013) which we use. A magnetostratigraphy-based age model defined the placement of this cooling event at 27.91 Ma (Wade and Pälike, 2004), supporting that the Oi-2a event is associated with the hiatus between Sequence O6 and O3, too.

The placement of the Mi-1 event for the New Jersey margin and the NJSS is difficult and not unequivocal. Kotthoff et al. (2014) suggested, based on a lower resolution NJSS record from Site M0027, that the Mi-1 event is reflected at a depth of ~530 mbsf, after the onset of Sequence O6. This is supported by the data of Browning et al. (2013, fig. 7 therein) where Sequence O6 comprises the Mi-1 event. Our higher-resolution analysis shows a temperature decrease around this depth, and a peak in high altitude forest taxa, e.g., *Picea* as wall as a peak in the presumed lowland conifer *Cathaya*, with maxima at ~535 mbsf (Figs. 3, 4). But in contrast to Kotthoff et al. (2014), we suggest that these signals might rather reflect a cooling event during the Mi-1 onset. Antarctic ice sheet expansion during the Mi-1 event likely caused the sequence boundary between Sequences O6 and m6 at ~510 at NJSS (Figs. 2 and 3; Browning et al., 2013). Such a scenario would be consistent with Pekar et al. (2002), who placed the Mi-1 event at the New Jersey margin also between these sequences, reconstructing an apparent sea-level drop of 56 m.

Age estimations for the hiatus between Sequences O6 and m6 differ between the records from the New Jersey margin (Pekar et al., 2002) and the NJSS (Browning et al., 2013). According to Browning et al. (2013), the top of Sequence O6 is dated to 23.0 Ma for Site M0027 from the NJSS, which would still almost fit with the general placement of the Mi-1 event and thus the OMB at 23.03 Ma (e.g., GTS2012; Gradstein et al., 2012; Cohen et al., 2016), a time during which Antarctica experienced maximum ice volume (Zachos et al., 2001; Liebrand et al., 2011). For the New Jersey margin however (e.g., Pekar et al., 2002), the top of Sequence O6 is dated to 23.8 Ma. While it is possible that Sequence O6 may be slightly younger at the NJSS (Browning et al., 2013), this is still a significant discrepancy. It must be noted though that the general placement of the OMB is based on different age control techniques, e.g. orbital tuning (e.g., Liebrand et al., 2011) than its placement at the NJSS, which is based on Sr isotope stratigraphy (supported by biostratigraphy, e.g., calcareous nannoplankton and dinoflagellate cyst occurrences) with considerable errors of up to 0.5 Ma. Similarly, the age model for records from the New Jersey margin (Miller et al., 1998; Pekar et al., 2002), also based on Sr isotopy, have errors up to 0.6 Ma for the time interval around the OMB.

While our new record does not indicate a significant increase of high −/medium-altitude forest taxa at the end of Sequence O6, our climate data indicates a temperature decrease just before the hiatus between Sequences O6 and m6 which might reflect the onset of the Mi-1 event (compare Section 4.4.2). The uncertainty of the temporal placement of the Mi-1 event and its local terrestrial imprint of the New Jersey hinterland needs further detailed analysis. Subsequently, other cooler environmental basic conditions occurred within Sequence m6 (~20.9 to 20.7 Ma; Fig. 4) and probably reflect a late Aquitanian vegetation change provoked by an unnamed event, which is expressed in a $\delta^{18}O$ increase at ~20.8 Ma (Browning et al., 2013).

4.4.2. Regional altitudinal paleoenvironmental changes

Across the analyzed time interval several potential topographic vegetation movement signals can be linked to climatic deterioration events of the Oligocene. These signals are primarily visible in peaks of relative abundances of bisaccate pollen grains produced by *Pinus*, *Picea* and *Cathaya* (Fig. 3). Those taxa probably show the highest sensitivity and apparently benefitted from the changing environmental conditions of the Oligocene.

The relatively low amount of *Pinus* and *Picea* pollen grains over long intervals in our record may point to a generally distant source area, more likely the mid- and high-altitude forests than lower elevation or shoreline areas. Lowland paleoforest communities dominated by *Pinus* spp. document exceptionally high amounts of *Pinus* pollen grains (e.g., Stolze et al., 2007; Kotthoff et al., 2008). However, we cannot rule out that single *Pinus* species may have colonized lowland habitats as well.

The first peaks of relative abundances of *Pinus* and *Cathaya* (Fig. 2; Fig. 4) from ~29.3 to ~29.0 Ma (~610 to ~595 mbsf) might be the impact of the unnamed $\delta^{18}O$ excursion or respectively the Oi-2* event which took place ~29.1 Ma (Pekar et al., 2002; Wade and Pälike, 2004). For this time interval, a considerable high amount of bisaccate pollen grains was recognized (Fig. 4), which does not correspond with the P:D ratio. Therefore, a solely associated taphonomic transport effect can be excluded. This indicates the earliest downslope movement signal of *Pinus* spp. and an expansion of lowland *Cathaya* within the mixed mesophytic forest on wet/moist soils (Fig. 3) in the New Jersey hinterland in our record. Pollen grains of *Picea*, *Abies* and *Larix*/*Pseudotsuga* were only sporadically found in the early Oligocene sediments. The conifers spread into the lowland and partly replaced the mesophytic forest growing on well drained soils (Fig. 4). The idea of downward movement of the conifers is again reinforced by the negatively correlating P:D ratio, which indicates an increasing shoreline vicinity and thus only a low possibility of transport-induced increase in bisaccate pollen percentages. Relative pollen abundances of the mesophytic forest growing on well-drained soils, however, remained relative stable (Fig. 4), indicating that either the amplitude of climatic factors (e.g., cooling) was too small to induce a strong reduction of the mesophytic forest or rather that the regional terrestrial ecosystem had a high degree of resilience to the climate forcing, since our climate reconstructions indicate significant declines in temperature around this time (Fig. 5).

The first notable decline of pollen grains assigned to the mesophytic forest growing on well-drained soils occurred around tintrasequence reflector o.5 (~570 to ~560 mbsf, ~28.3 Ma, Fig. 4; compare Browning et al., 2013). This decline is simultaneously accompanied by a pollen grain increase of *Larix*/*Pseudotsuga*, *Abies*, *Picea*, *Pinus* and *Cathaya* (Fig. 3). It is difficult to assign this decline to events reflected at the New Jersey margin (e.g., Pekar et al., 2002) due to the differences in the age models. Compared to the Oligocene record from the Pacific presented by Wade and Pälike (2004), the cooling signal from the NJSS would rather fall after the Oi-2* event and before the subsequent Oi-2a event and might reflect a cooling phase in between, during an interval of particularly strong obliquity changes. Such a phase is indeed indicated in the record from the Pacific at ~28.3 Ma (Wade and Pälike, 2004). This appears reasonable considering that the Oi-2a event itself is probably not reflected in our record (see above).

The highest input of pollen of typical cold-tolerant genera such as *Picea*, *Abies* (Fig. 3), together with *Pinus* and *Cathaya* pollen is documented at the onset of Sequence O6 (~535 mbsf, ~23.5 Ma). Abiotic factors presumably promoted the expansion of conifers, which is consistent with findings of Kotthoff et al. (2014), even though we dismiss their correlation to the Mi-1 event (see Section 4.4.1). The Oi-2c

event at around 25.8 Ma mentioned by Pekar et al. (2002) does fit stratigraphically with the increase of cold-tolerant taxa at NJSS and an increase in the $\delta^{18}O$ record from Site 1218 from the Pacific at ~23.4 Ma (Pälike et al., 2006), which is followed by the transition into the OMB. The increase of pollen grains assigned to the mid- and high-altitude conifer forest led to a relative decrease of the mesophytic forest growing on dry soil. The relationship between the decrease of relative abundances of mesophytic forest growing on dry soil and the reduction of the oak population (Figs. 3 and 4) is emphasized by Kotthoff et al. (2014). A subsequent temperature drop is indicated within all parameters at ~530 mbsf, with a stepwise MAT-decline of ~3 °C. This temperature drop probably matches the MAT-drop of ~4 °C described by Kotthoff et al. (2014) at the same depth. It should be noted that the temperature decrease in our study is based on the absence of the thermophilous taxon *Gordonia*, which was present in samples below and above ~530 mbsf. A coeval increase of plant communities associated with coastal environments, growing on sun-exposed sandbanks, such as *Ephedra*, probably reflecting drier and cooler conditions (Fig. 3), is also consistent with Kotthoff et al. (2014). However, MAP does not decrease around this interval; the estimates rather suggest an overall stability.

Slightly higher values of high- and mid-altitude conifer forest pollen around the Mi-1 hiatus at 510 mbsf at NJSS, compared to particularly low values before (around ~517 mbsf), suggest that these forest types had already started to spread prior to the cooling, but these signals are weak compared to other increases discussed above.

Generally, the mesophytic forest growing on moist/wet soils of the New Jersey hinterland is in phase with depositional changes of the Oligocene and early Miocene sedimentary succession at Site M0027 and indirectly confirms climate and sea-level change. During regressive phases (glacial phases) and downslope conifer forest expansion, shallow shelf areas were exposed, allowing substrate-depending forest formation closer to the coring site (Fig. 3). Concomitant increases of the (H (s))-Index indicate a quite diverse low elevation forest and thus a decreasing distance to the shoreline, facilitating pollen grain input during regression phases and/or a larger altitudinal gradient.

No further information of macrofloristic remains of Cupressaceae are reported from deposits of the North American Atlantic east coast (e.g., Tiffney, 1994). The Cupressaceae contains genera which are highly variable in their ecological range (Farjon, 2010). *Taiwania* (Taxodioideae) is currently restricted to higher elevated areas as part of the conifer forest belt in Asia (Farjon, 2010), growing under generally warm conditions but tolerant of occasional cold phases (LePage, 2009). During the Cenozoic it was widespread across the Northern Hemisphere (LePage, 2009). Similar to *Cathaya*, *Taiwania* might also have flourished in the swampy lowland landscapes of the hinterland as it is evident from Central Europe, were in situ fossilized wood in were found brown coal fields (Dolezych and Schneider, 2007). A portion of the Cupressaceae pollen grains with a papilla recorded at the NJSS might have been produced by *Taiwania* (Hernandez-Castillo et al., 2005).

The simultaneous increases of Cupressaceae and *Pinus*, *Cathaya* and *Picea* pollen grains potentially link and reinforce their expansion as a direct response to environmental changes related to cooling. *Taxodium* sp. macro-remains (leafs, fruits seeds) are also present in the Miocene Brandywine deposit in southern Maryland (McCartan et al., 1990).

5. Conclusions

This study revealed high values of mesic forest taxa in the New Jersey hinterland during the Oligocene and early Miocene. Bioclimatic analysis reflects humid and warm temperate conditions during the recovered sea-level high stand phases, and reveals a long-term relative climatic stability during the middle Oligocene to early Miocene.

The relatively high abundances of *Quercus* pollen grains emphasize the dominance and significance of this taxon within the mesophytic forest. The presence of different pollen grain sculptures suggests a diverse *Quercus* population at sectional level and most likely represents section *Quercus, Lobatae*, *Quercus/Lobatae* and aff. section *Protobalanus*. The sporadic occurrence of the extinct Fagaceae genus *Eotrigonobalanus* in the New Jersey hinterland extends the view of its distribution the Northern Hemisphere during the Cenozoic.

The limited temporal resolution and age control of our pollen record from the NJSS inhibits the evaluation of vegetation responses to periodic orbital changes of the Oligocene and early Miocene. Nevertheless, the terrestrial palynomorph abundances demonstrate repeated fluctuations on time scales of 10^4–10^5 years, likely representing downslope vegetation shifts, consistent with cooling. Some, but not all, of these fluctuations are associated with temperature and humidity declines based on the bioclimatic analysis.

The downward expansion of mid- and high-altitude conifer forest during cooling phases coincides with a certain replacement of the mesophytic forest growing on dry soils, revealing a direct cooling signal. Regression phases (glacial phases) exposed shallow shelf areas and allowed the expansion of substrate-depending forest formations. The spread of the Cupressaceae and the mixed mesophytic forest growing on moist or wet soils during glacial phases thus represents an indirect confirmation of climate change.

We relate peaks of relative abundances of *Pinus* and *Cathaya* from ~29.3 to ~29.0 Ma to an unnamed $\delta^{18}O$ excursion at ~29.1 Ma reported from the New Jersey margin and, termed as Oi-2*, from the tropical Pacific. Several cooling events such as the Oi2-a event are probably concealed in our record due to an interruption of sedimentation between ~28.3 and 23.5 Ma.

In contrast to Kotthoff et al. (2014), we suggest that the MAT decline and conifer peak in our record during Sequence O6 from the New Jersey Shelf (~23.5 to ~23.0 Ma) reflects a cooling event during a phase of high sea level, and not of the Mi-1 event. Instead, a second stronger MAT decrease, just before the hiatus between Sequences O6 and m6, probably is the onset of the Mi-1 event, while the event itself is reflected by a hiatus between the sequences between ~23.0 and ~20.9 Ma. Considering the Sr-isotopy-related dating uncertainties, this agrees with the Mi-1 age of 23.05 Ma.

Subsequent indications for relatively cooler environmental conditions between ~20.9 and 20.7 Ma probably reflect a late Aquitanian vegetation change provoked by an unnamed event which is expressed in a $\delta^{18}O$ increase at ~20.8 Ma.

Data availability

Data will be uploaded at Pangea and at the Research Data Repository FDR@UHH (Hamburg University). Palynological slides will be stored at the Center of Natural History (Hamburg University).

Declaration of Competing Interests

The authors declare that they have no known competing financial interests or personal relationships that could have appeared to influence the work reported in this paper.

Acknowledgements

We thank the entire Integrated Ocean Drilling Program (IODP) Expedition 313 Scientific Party and the staff of the IODP Core Repository Bremen. We acknowledge A. Krueger, Palynology Lab at Brock University; E. Czymoch and K. A. Harps, University of Hamburg, for sample processing and Y. Milker, M. Theodor and R. Walter, for support at the SEM, J. Reolid and K. Miller for animating discussion, T. Denk for his highly useful comments on an earlier draft of this manuscript, and M. Finotti for technical support. The research was supported by the German Research Foundation [DFG; Project Ko 3944/5]. DRG's participation was further supported by a grant from the Natural Sciences and Engineering Research Council of Canada [2016-04337].

Appendix A. Supplementary data

Supplementary data to this article can be found online at https://doi.org/10.1016/j.revpalbo.2020.104224.

References

Abrams, M.D., 1992. Fire and the development of Oak Forests. BioScience. 42, 346–353.

Barrón, A., Zobaa, M.K., Oboh-Ikuenobe, F.E., 2017. Palynological evidence for sustained deep-marine conditions during the Eocene–Miocene in the southern Gulf of Mexico distal continental margin. Geol. Soc. Am. Bull. 129, 218–228.

Bates, C.D., Coxon, P., Gibbard, P.L., 1978. A new method for the preparation of clay-rich sediment samples for palynological investigation. New Phytol. 81, 459–463.

Bouchal, J., Zetter, R., Grímsson, F., Denk, T., 2014. Evolutionary trends and ecological differentiation in early Cenozoic Fagaceae of western North America. Am. J. Bot. 101, 1–18.

Browning, J.V., Miller, K.G., Sugarman, P.J., Barron, J., McCarthy, F.M.G., Kulhanek, D.K., Katz, M.E., Feigenson, M.D., 2013. Chronology of Eocene-Miocene sequences on the New Jersey shallow shelf: Implications for regional, interregional, and global correlations. Geosphere 9, 1434–1456.

Bůzek, Č., Kvaček, Z., Manchester, S.R., 1989. Sapindaceous affinities of the *Pteleaecarpum* fruits from the tertiary of Eurasia and North America. Bot. Gaz. 150, 477–489.

Cavender-Bares, J., Ackerly, D.D., Baum, D.A., Bazzaz, F.A., 2004. Phylogenetic overdispersion in Floridian oak communities. Am. Nat. 163, 823–843.

Cavender-Bares, J., Gonzalez-Rodriguez, A., Pahlich, A., Koehler, K., Deacon, N., 2011. Phylogeography and climatic niche evolution in live oaks (*Quercus series Virentes*) from the tropics to the temperate zone. J. Biogeogr. 38, 962–981.

Cavender-Bares, J., González-Rodríguez, A., Eaton, D.A.R., Hipp, A.A.L., Beulke, A., Manos, P.S., 2015. Phylogeny and biogeography of the American live oaks (*Quercus* subsection *Virentes*): A genomic and population genetics approach. Mol. Ecol. 24, 3668–3687.

Cohen, K.M., Finney, S.C., Gibbard, P.L., Fan, J.X., 2016. The ICS international chronostratigraphic chart. Episodes 36, 199–204 (2013: updated).

Coxall, H.K., Wilson, P.A., Palike, H., Lear, C.H., Backman, J., 2005. Rapid stepwise onset of Antarctic glaciation and deeper calcite compensation in the Pacific Ocean. Nature 433, 53–57.

Crepet, W.L., Nixon, K.C., 1989. Extinct transitional Fagaceae from the Oligocene and their phylogenetic implications. Am. J. Bot. 76, 1493–1505.

Denk, T., 2003. Phylogeny of *Fagus* L. (Fagaceae) based on morphological data. Plant Syst. Evol. 240, 55–81.

Denk, T., Grimm, G.W., 2009a. Significance of Pollen Characteristics for Infrageneric Classification and Phylogeny in Quercus (Fagaceae). Int. J. Plant Sci. (170), 926–940.

Denk, T., Grimm, G.W., 2009b. The biogeographic history of beech trees. Rev. Palaeobot. Palynol. 158, 83–100.

Denk, T., Grimm, G.W., Hemleben, V., 2005. Patterns of molecular and morphological differentiation in *Fagus* (Fagaceae): Phylogenetic implications. Am. J. Bot. 92, 1006–1016.

Denk, T., Grímsson, F., Zetter, R., 2010. Episodic migration of oaks to Iceland: Evidence for a North Atlantic "land bridge" in the latest Miocene. Am. J. Bot. 97, 276–287.

Denk, T., Grímsson, F., Zetter, R., 2012. Fagaceae from the early Oligocene of Central Europe: Persisting new world and emerging old world biogeographic links. Rev. Palaeobot. Palynol. 169, 7–20.

Denk, T., Grimm, G.W., Deng, M., Hipp, A.L., 2017. In: Gil-Pelegrín, E., Peguero-Pina, J.J., Sancho-Knapik, D. (Eds.), An updated infrageneric classification of the oaks: Review of previous taxonomic schemes and synthesis of evolutionary patterns. Springer International Publishing AG, Oaks Physiological Ecology. Exploring the Functional Diversity of Genus Quercus L, pp. 13–38.

Dolezych, M., Schneider, W., 2006. Inkohlte Hölzer und Cuticulae dispersae aus dem 2. Miozänen Flözhorizont im Tagebau Welzow (Lausitz) – Taxonomie und vergleichende feinstratigraphisch-fazielle Zuordnung. Z. Geol. Wiss. 34, 165–259.

Dolezych, M., Schneider, W., 2007. Taxonomie und Taphonomie von Koniferenhölzern und Cuticulae dispersae im 2. Lausitzer Flözhorizont (Miozän) des Senftenberger Reviers. Palaeontograph. B 276, 1–95.

Dolezych, M., Schneider, W., 2012. Fossil conifers in peat bog environments – results from the Central European Neogene. Japan. J. Palynol. 58 (Special issue), 48.

Donders, T.H., van Helmond, N.A.G.M., Verreussel, R., Munsterman, D., ten Veen, J., Speijer, R.P., Weijers, J.W.H., Sangiorgi, F., Peterse, F., Reichart, G.J., Sinninghe Damsté, J.S., Lourens, L., Kuhlmann, G., Brinkhuis, H., 2018. Land–sea coupling of early Pleistocene glacial cycles in the southern North Sea exhibit dominant Northern Hemisphere forcing. Clim. Past 14, 397–411.

eFloras, 2008. Flora of North America. http://www.efloras.org accessed March–June 2017.

Eldrett, J.S., Greenwood, D.R., Harding, I.C., Huber, M., 2009. Increased seasonality through the Eocene to Oligocene transition in northern high latitudes. Nature 459, 969–973.

Fang, J., Wang, Z., Tang, Z., 2011. Atlas of Woody Plants in China: Distribution and Climate. Volume 1. Springer, Higher Education Press, Beijing.

Farjon, A., 2010. A Handbook of the World's Conifers. Volumes 1 and 2. Leiden, Brill Academic Pub.

Frederiksen, N.O., 1980. Mid-Tertiary climate of Southeastern United States: The sporomorph evidence. J. Paleontol. 54, 728–739.

Frederiksen, N.O., 1991. Pulses of Middle Eocene to earliest Oligocene climatic deterioration in Southern California and the Gulf Coast. Palaios 6, 564–571.

Global Biodiversity Information Facility (GBIF), 2001. http://www.gbif.org, last access: May, 2012.

Goldner, A., Huber, M., Caballero, R., 2013. Does Antarctic glaciation cool the world? Clim. Past 9, 173–189.

Gradstein, F.M., Ogg, J.G., Hilgen, F.J., 2012. On the geologic time scale. Newsl. Stratigr. 45, 171–188.

Graham, A., 1999. Late Cretaceous and Cenozoic History of North Amercian Vegetation. Oxford University Press, New York.

Greenwood, D.R., Archibald, S.B., Mathewes, R.W., Moss, P.T., 2005. Fossil biotas from the Okanagan Highlands, southern British Columbia and northeastern Washington State: Climates and ecosystems across an Eocene landscape. Can. J. Earth Sci. 42, 167–185.

Grimm, G., Denk, T., Bouchal, J.M., Potts, A.J., 2015. Fables and foibles: a critical analysis of the Palaeoflora database and the Coexistence approach for palaeoclimate reconstruction. BioRxiv https://doi.org/10.1101/016378.

Grímsson, F., Grimm, G.W., Zetter, R., Denk, T., 2016. Cretaceous and Paleogene Fagaceae from North America and Greenland: Evidence for a Late Cretaceous split between *Fagus* and the remaining Fagaceae. Acta Palaeobot. 56, 247–305.

Grímsson, F., Zetter, R., 2011. Combined LM and SEM study of the Middle Miocene (Sarmatian) palynoflora from the Lavanttal Basin, Austria: Part II. Pinophyta (Cupressaceae, Pinaceae and Sciadopityaceae). Grana 50, 262–310.

Grímsson, F., Zetter, R., Grimm, G.W., Pedersen, G.K., Pedersen, A.K., Denk, T., 2015. Fagaceae pollen from the early Cenozoic of West Greenland: Revisiting Engler's and Chaney's Arcto-Tertiary hypotheses. Plant Syst. Evol. 301, 809–832.

Grímsson, F., Grimm, G.W., Meller, B., Bouchal, J.M., Zetter, R., 2016b. Combined LM and SEM study of the middle Miocene (Sarmatian) palynoflora from the Lavanttal Basin, Austria: Part IV. Magnoliaphytina 2 – Fagales to Rosales. Grana. 55, 101–163.

Hably, L., Kvaček, Z., Manchester, S.R., 2000. Shared taxa of land plants in the Oligocene of Europe and North America in context of Holarctic Phytogeography. Acta Univ. Carol. Geol. 44, 59–74.

Herbert, J., 2005. Systematics and biogeography of Myricaceae. PhD thesis. University of St Andrews, St Andrews, UK.

Herendeen, P.S., Crepet, W.L., Nixon, K.C., 1994. Fossil flowers and pollen of Lauraceae from the Upper Cretaceous of New Jersey. Plant Syst. Evol. 189, 29.

Hernandez-Castillo, G.R., Stockey, R.A., Beard, G., 2005. Taxodiaceous pollen cones from the Early Tertiary of British Columbia, Canada. Int. J. Plant Sci. 166, 339–346.

Hesse, M., Halbritter, H., Zetter, R., Weber, M., Buchnerm, R., Frosch-Radivo, A., Ulrich, S., 2009. Pollen Terminology – An Illustrated Handbook. Springer, Wien.

Hipp, A.L., Manos, P.S., Hahn, M., Avishai, M., Bodénès, C., Cavender-Bares, J., Crowl, A.A., Deng, M., Denk, T., Fitz-Gibbon, S., Gailing, O., González-Elizondo, M.S., González-Rodríguez, A., Grimm, G.W., Jiang, X.-L., Kremer, A., Lesur, I., McVay, J.D., Plomion, C., Rodríguez-Correa, H., Schulze, E.-D., Simeone, M.C., Sork, V.L., Valencia-Avalos, S., 2019. Genomic landscape of the global oak phylogeny. New Phytol. https://doi.org/10.1111/nph.16162.

Hofmann, C.C., Gregor, H.J., 2018. Scanning electron microscope and light microscope investigations of pollen from an atypical mid-Eocene coal facies in Stolzenbach mine (PreußenElektra) near Borken (Kassel, Lower Hesse, Germany). Rev. Palaeobot. Palynol. 252, 41–63.

Kmenta, M., Zetter, R., 2013. Combined LM and SEM study of the upper Oligocene/lower Miocene palynoflora from Altmittweida (Saxony): Providing new insights into Cenozoic vegetation evolution of Central Europe. Rev. Palaeobot. Palynol. 195, 1–18.

Korasidis, V.A., Wallace, M.W., Wagstaff, B.E., Hill, R.S., 2019. Terrestrial cooling record through the Eocene-Oligocene transition of Australia. Glob. Planet. Chang. 173, 61–72.

Kotthoff, U., Müller, U.C., Pross, J., Schmiedl, G., Lawson, I.T., van de Schootbrugge, B., Schulz, H., 2008. Late Glazial and Holocene vegetation dynamics in the Aegean region: An integrated view based on pollen data from the marine and terrestrial archives. Holocene 18, 1019–1032.

Kotthoff, U., Greenwood, D.R., McCarthy, F.M.G., Müller-Navarra, K., Prader, S., Hesselbo, S.P., 2014. Late Eocene to middle Miocene (33 to 13 million years ago) vegetation and climate development on the North American Atlantic Coastal Plain (IODP Expedition 313, Site M0027). Clim. Past 10, 1523–1539.

Kovar-Eder, J., 2016. Early Oligocene plant diversity along the Upper Rhine Graben: The fossil flora of Rauenberg, Germany. Acta Palaeobot. 56, 329–440.

Kvaček, Z., 2007. Do extant nearest relatives of thermophile European Cenozoic plant elements reliably reflect climatic signal? Palaeogeogr. Palaeoclimatol. Palaeoecol. 253, 32–40.

Kvaček, Z., Walther, H., 1991. Revision der mitteleuropäischen tertiären Fagaceen nach blattepidermalen Charakteristiken. IV. Teil Fagus Linné. Feddes Repert. 102, 471–534.

Kvaček, Z., Manchester, S.R., Zetter, R., Pingen, M., 2002. Fruits and seeds of Craigia bronnii (Malvaceae – Tilioideae) and associated flower buds from the late Miocene Inden Formation, Lower Rhine Basin, Germany. Rev. Palaeobot. Palynol. 119, 311–324.

Larsson, L.M., Dybkjær, K., Rasmussen, E.S., Piasecki, S., Utescher, T., Vajda, V., 2011. Miocene climate evolution of northern Europe: A palynological investigation from Denmark. Palaeogeogr. Palaeoclimatol. Palaeoecol. 309, 161–175.

Lear, C.H., Rosenthal, Y., Coxall, H.K., Wilson, P.A., 2004. Late Eocene to early Miocene ice sheet dynamics and the global carbon cycle. Paleoceanography 19, PA4015. https://doi.org/10.1029/2004PA001039.

LePage, B.A., 2009. Earliest occurrence of *Taiwania* (Cupressaceae) from the Early Cretaceous of Alaska: Evolution, biogeography, and paleoecology. Proc. Acad. Nat. Sci. Phila. 158, 129–158.

Liebrand, D., Lourens, L.J., Hodell, D.A., de Boer, B., van de Wal, R.S.W., Pälike, H., 2011. Antarctic ice sheet and oceanographic response to eccentricity forcing during the early Miocene. Clim. Past 7, 869–880.

Liu, L., 2014. Rejuvenation of Appalachian topography caused by subsidence-induced differential erosion. Nat. Geosci. 7, 518–523.
Liu, Y.S., Basinger, J.F., 2000. Fossil *Cathaya* (Pinaceae) pollen from the Canadian High Arctic. Int. J. Plant Sci. 161, 829–847.
Lott, T.A., Manchester, S.R., Corbett, S.L., 2019. The Miocene flora of Alum Bluff, Liberty County, Florida. Acta Palaeobot. 59 (1), 75–129.
Manchester, S.R., 1987. The fossil history of the Juglandaceae. Monogr. Syst. Bot. 21.
Manchester, S.R., 1994. Fruits and seeds of the Middle Eocene Nut Beds flora, Clarno Formation, Oregon. Palaeontogr. Am. 58, 1–205.
Manchester, S.R., 1999. Biogeographical relationships of North American Tertiary floras. Ann. Mo. Bot. Gard. 86, 472–522.
Manchester, S.R., 2011. Fruits of Ticodendraceae (Fagales) from the Eocene of Europe and North America. Int. J. Plant Sci. 172, 1179–1187.
Mawbey, E.M., Lear, C.H., 2013. Carbon cycle feedbacks during the Oligocene–Miocene transient glaciation. Geology 41, 963–966.
McCartan, L., Tiffney, B.H., Wolfe, J.A., Ager, T.A., Wing, S.L., Sirkin, L.A., Ward, L.W., Brooks, J., 1990. Late Tertiary floral assemblage from upland gravel deposits of the southern Maryland Coastal Plain. Geology 18, 311–314.
McCarthy, F.M.G., Gostlin, K.E., Mudie, P.J., Hopkins,J., 2003. Terrestrial and marine palynomorphs as sea-level proxies: An example from Quaternary sediments on the New Jersey margin. In Olson, H.C., Leckie, M., (Eds.), Micropaleontologic Proxies for Sea-Level Change and Stratigraphic Discontinuities. SEPM Special Publication No. 75, 119–129.
McCarthy, F.M.G., Mudie, P.J., 1998. Oceanic pollen transport and pollen:dinocyst ratios as markers of late cenozoic sea level change and sediment transport. Palaeogeogr. Palaeoclimatol. Palaeoecol. 138, 187–206.
McCarthy, F.M.G., Katz, M.E., Kotthoff, U., Browning, J.V., Miller, K.G., Zanatta, R., Williams, R.H., Drljepan, M., Hesselbo, S.P., Bjerrum, C.J., Mountain, G.S., 2013. Sea-level control of New Jersey margin architecture: Palynological evidence from Integrated Ocean Drilling Program Expedition 313. Geosphere 9, 1457–1487.
Meyer, H.W., Manchester, S.R., 1997. The Oligocene Bridge Creek Flora of the John Day Formation, Oregon. University of California Publications in Geological Sciences, Berkeley, Los Angeles, London.
Miller, K.G., Mountain, G.S., Browning, J.V., Komiz, M., Sugarman, P.J., Christie-Blick, N., Katz, M.E., Wright, J.D., 1998. Cenozoic global sea level, sequences, and the New Jersey Transect: Results From coastal plain and continental slope drilling. Rev. Geophys. (36), 569–601 https://doi.org/10.1029/98RG01624.
Miller, K.G., Browning, J.V., Mountain, G.S., Bassetti, M.A., Monteverde, D., Katz, M.E., Inwood, J., Lofi, J., Proust, J.N., 2013a. Sequence boundaries are impedance contrasts: Core-seismic-log integration of Oligocene–Miocene sequences, New Jersey shallow shelf. Geosphere 9, 1257–1285.
Miller, K.G., Mountain, G.S., Browning, J.V., Katz, M.E., Monteverde, D., Sugarman, P.J., Ando, H., Bassetti, M.A., Bjerrum, C.J., Hodgson, D., Hesselbo, S., Karakaya, S., Proust, J.N., Rabineau, M., 2013b. Testing sequence stratigraphic models by drilling Miocene foresets on the New Jersey shallow shelf. Geosphere 9, 1236–1256.
Mountain, G.S., Proust, J.N., McInroy, D., Cotterill, C., the Expedition 313 Scientists, 2010. Proceedings of the Integrated Ocean Drilling Program. Expedition 313. Integrated Ocean Drilling Program Management International, Inc, Tokyo.
Mudie, P.J., McCarthy, F.M.G., 1994. Late Quaternary pollen transport processes, western North Atlantic: Data from box models, cross-margin and N-S transects. Mar. Geol. 118, 79–105.
Mudie, P.J., McCarthy, F.M.G., 2006. Marine palynology: potentials for onshore—offshore correlation of Pleistocene—Holocene records. Trans. R. Soc. S. Afr. 61, 139–157.
Naish, T.R., Woolfe, K.J., Barrett, P.J., Wilson, G.S., Atkins, C., Bohaty, S.M., Bucker, C.J., Claps, M., Davey, F.J., Dunbar, G.B., Dunn, A.G., Fielding, C.R., Florindo, F., Hannah, M.J., Harwood, D.M., Henrys, S.A., Krissek, L.A., Lavelle, M., van der Meer, J., McIntosh, W.C., Niessen, F., Passchier, S., Powell, R.D., Roberts, A.P., Sagnotti, L., Scherer, R.P., Strong, C.P., Talarico, F., Verosub, K.L., Villa, G., Watkins, D.K., Webb, P.N., Wonik, T., 2001. Orbitally induced oscillations in the East Antarctic ice sheet at the Oligocene/Miocene boundary. Nature 413, 719–723.
Natural Resources Canada, 2001. Climatic Range Map (1971-2000scenario)/Climatic Profile: Canadian Forest Service, Sault Ste. Marie. http://planthardiness.gc.ca/index.pl?lang=enandm=13anddp=1. last access: May 2012.
Oboh, F.E., Reeves Morris, L.M., 1994. Early Oligocene Palynosequences in the Eastern Gulf Coast, U.S.A. Palynology 18, 213–235.
Oboh, F.E., Jaramillo, C.A., Reeves Morris, L.M., 1996. Late Eocene-Early Oligocene paleofloristic patterns in southern Mississippi and Alabama, US Gulf Coast. Rev. Palaeobot. Palynol. 91, 23–34.
Pagani, M., Zachos, J.C., Freeman, K.H., Tipple, B., Bohaty, S., 2005. Marked decline in atmospheric carbon dioxide concentrations during the Paleogene. Science 309, 600–603.
Pälike, H., Norris, R.D., Herrle, J.O., Wilson, P.A., Coxall, H.K., Lear, C.H., Shackleton, N.J., Tripati, A.K., Wade, B.S., 2006. The heartbeat of the Oligocene climate system. Science 314, 1894–1898.
Pekar, S.F., Miller, K.G., 1996. New Jersey Oligocene "Icehouse" sequences (ODP Leg 150X) correlated with global d18O and Exxon eustatic records. Geology 24, 567–570.
Pekar, S.F., Christie-Blick, N., Kominz, M.A., Miller, K.G., 2002. Calibration between eustatic estimates from backstripping and oxygen isotopic records for the Oligocene. Geology 30, 903–906.
Pekar, S.F., DeConto, R.M., Harwood, D.M., 2006. Resolving a late Oligocene conundrum: Deep-sea warming and Antarctic glaciation. Palaeogeogr. Palaeoclimatol. Palaeoecol. 231, 29–40.
Potonié, R., 1931. Zur Mikroskopie der Braunkohlen. Tertiäre Blütenstaubformen. Braunkohle 30, 325–333.
Pound, M.J., Salzmann, U., 2017. Heterogeneity in global vegetation and terrestrial climate change during the late Eocene to early Oligocene transition. Sci. Rep. 7, 43386. https://doi.org/10.1038/srep43386.
Prader, S., Kotthoff, U., McCarthy, F.M.G., Schmiedl, G., Donders, T.H., Greenwood, D.R., 2017. Vegetation and climate development of the New Jersey hinterland during the late Middle Miocene (IODP Expedition 313 Site M0027). Palaeogeogr. Palaeoclimatol. Palaeoecol. 485, 854–868.
Prebble, J.G., Reichgelt, T., Mildenhall, D.C., Greenwood, D.R., Raine, J.I., Kennedy, E.M., Seebeck, H.C., 2017. Terrestrial climate evolution in the Southwest Pacific over the past 30 million years. Earth Planet. Sci. Lett. 459, 136–144.
Retallack, G.J., Orr, W.N., Prothero, D.R., Duncan, R.A., Kester, P.R., Ambers, C.P., 2004. Eocene-Oligocene extinction and paleoclimatic change near Eugene. Oregon. Geol. Soc. Am. Bull. 116, 817–839.
Roth-Nebelsick, A., Oehm, C., Grein, M., Utescher, T., Kunzmann, L., Friedrich, J.P., Konrad, W., 2014. Stomatal density and index data of *Platanus neptuni* leaf fossils and their evaluation as a CO2 proxy for the Oligocene. Rev. Palaeobot. Palynol. 206, 1–9.
Scher, H.D., Martin, E.E., 2006. Timing and climatic consequences of the opening of Drake passage. Science 312, 428–430.
Schlitzer, R., 2011. Ocean Data View. http://odv.awi.de.
Scotese, C.R., Gahagan, L.M., Larson, R.L., 1988. Plate tectonic reconstructions of the Cretaceous and Cenozoic ocean basins. Tectonophysics 155, 27–48.
Stolze, S., Roe, H.M., Patterson, R.T., Monecke, T., 2007. A record of Lateglacial and Holocene vegetation and climate change from Woods Lake, Seymour Inlet, coastal British Columbia, Canada. Rev. Palaeobot. Palynol. 147, 112–127.
Strömberg, C.A.E., 2005. Decoupled taxonomic radiation and ecological expansion of open-habitat grasses in the Cenozoic of North America. Proc. Nat. Acad. Sci. 102, 11980–11984.
Thompson, R.S., Anderson, K.H., Bartlein, P.J., 2000a. Atlas of relations between climatic parameters and distributions of important trees and shrubs in North America: Hardwoods. U.S. Geol. Surv. Prof. 1650-B.
Thompson, R.S., Anderson, K.H., Bartlein, P.J., Smith, S.A., 2000b. Atlas of relations between climatic parameters and distributions of important trees and shrubs in North America: additional conifers, hardwoods, and monocots. U.S. Geol. Surv. Prof. 1650-C.
Thompson, R.S., Anderson, K.H., Strickland, L.E., Shafer, S.L., Peltier, R.T., Bartlein, P.J., 2006. Atlas of relations between climatic parameters and distributions of important trees and shrubs in North America: Alaska species and ecoregions. U.S. Geol. Surv. Prof. 1650-D.
Thomson, P.W., Pflug, H., 1953. Pollen und Sporen des mitteleuropäischen Tertiärs. Palaeontographica 94 (B), 1–138.
Tiffney, B.H., 1977. Fruits and seeds of the Brandon Lignite: Magnoliaceae. Bot. J. Linn. Soc. 75, 299–323.
Tiffney, B.H., 1979. Fruits and seeds of the Brandon lignite III. Turpinia (Staphyleaceae). Brittonia 31, 39–51.
Tiffney, B.H., 1993. Fruits and seeds of the tertiary Brandon Lignite. VII. *Sargentodoxa* (Sargentodoxaceae). Am. J. Bot. 80, 517–523.
Tiffney, B.H., 1994. Re-evaluation of the age of the Brandon Lignite (Vermont, USA) based on plant megafossils. Rev. Palaeobot. Palynol. 82, 299–315.
Tiffney, B.H., Barghoorn, E.S., 1979. Flora of the Brandon Lignite. IV. Illiciaceae. Am. J. Bot. 66, 321–329.
Tiffney, B.H., Manchester, S.R., Fritsch, P.W., 2018. Two new species of *Symplocos* based on endocarps from the early Miocene Brandon Lignite of Vermont, USA. Acta Palaeobot. 58 (2), 185–198.
Traverse, A., 1955. Pollen analysis of the Brandon Lignite of Vermont. U.S. Dep. Inter., Bur. Mines, Rep. Invest. No. 5151, pp. 1–107.
Traverse, A., 1994. Palynofloral geochronology of the Brandon Lignite of Vermont, USA. Rev. Palaeobot. Palynol. 82, 265–297.
US Climate Data: https://www.usclimatedata.com; accessed November 2017.
Utescher, T., Bruch, A.A., Erdei, B., François, L., Ivanov, D., Jacques, F.M.B., Kern, A.K., Liu, Y.S., Mosbrugger, V., Spicer, R.A., 2014. The coexistence approach—Theoretical background and practical considerations of using plant fossils for climate quantification. Palaeogeogr. Palaeoclimatol. Palaeoecol. 410, 58–73.
Utescher, T., Bondarenko, O.V., Mosbrugger, V., 2015. The Cenozoic Cooling – continental signals from the Atlantic and Pacific side of Eurasia. Earth Planet. Sci. Lett. 415, 121–133.
van der Kaars, S., 2001. Pollen distribution in marine sediments from the south-eastern Indonesian waters. Palaeogeogr. Palaeoclimatol. Palaeoecol. 171, 341–361.
Velitzelos, E., Kvaček, Z., Walther, H., 1999. Erster Nachweis von *Eotrigonobalanus furcinervis* (Rossm.) Walther and Kvaček (Fagaceae) in Griechenland. Feddes Repert. 110, 349–358.
Velitzelos, D., Bouchal, J.M., Denk, T., 2014. Review of the Cenozoic floras and vegetation of Greece. Rev. Palaeobot. Palynol. 204, 56–117.
von der Heydt, A., Dijkstra, H.A., 2006. Effect of ocean gateways on the global ocean circulation in the late Oligocene and early Miocene. Paleoceanography 21, PA1011. https://doi.org/10.1029/2005PA00114.
Wade, B.S., Pälike, H., 2004. Oligocene climate dynamics. Paleoceanography 19. https://doi.org/10.1029/2004PA001042.
Walther, H., 2000. Floristic relationship between North and Central America and Europe in the Eocene. Acta Univ. Carol. Geol. 44, 51–57.
Walther, H., Zetter, R., 1993. Zur Entwicklung der paläogenen Fagaceae Mitteleuropas. Palaeontogr. B. 230, 183–194.
Wen, J., 1999. Evolution of Eastern Asian and Eastern North American disjunct distributions in flowering plants. Annu. Rev. Eco. Syst. 30, 421–455.

Williams, J.W., Shuman, B., Bartlein, P.J., Whitmore, J., Gajewski, K., Sawada, M., Minckley, T., Shafer, S., Viau, A.E., Webb III, T., Anderson, P.M., Brubaker, L.B., Whitlock, C., Davis, O.K., 2006. An Atlas of Pollen-Vegetation-Climate Relationships for the United States and Canada. American Association of Stratigraphic Palynologists Foundation, Dallas, TX, p. 293.

Willis, K.J., McElwain, J.C., 2014. The Evolution of Plants. Oxford University Press, Oxford.

Wolfe, J.A., Schorn, H.E., 1989. Paleoecologic, paleoclimatic, and evolutionary significance of the Oligocene Creede flora, Colorado. Paleobiology 15, 180–198.

Wolfe, J.A., Schorn, H.E., 1990. Taxonomic revision of the Spermatopsida of the Oligocene Creede flora, southern Colorado. U.S. Geol. Surv. Bull. Rep. No. 1923.

WorldClim, 2005. Global weather stations. http://www.worldclim.org. last access: May 2012.

Zachos, J.C., Shackleton, N.J., Revenaugh, J.S., Pälike, H., Flower, B.P., 2001. Climate response to orbital forcing across the Oligocene-Miocene boundary. Science 292, 274–278.

Zetter, R., Ferguson, D.K., 2001. Trapaceae pollen in the Cenozoic. Acta Palaeobot. 41, 321–339.

Zhang, J.B., Li, R.Q., Xiang, X.G., Manchester, S.R., Lin, L., Wang, W., Wen, J., Chen, Z.D., 2013. Integrated fossil and molecular data reveal the biogeographic diversification of the eastern Asian-eastern North American disjunct Hickory genus (*Carya* Nutt.). PLos One 8, e70449. https://doi.org/10.1371/journal.pone.0070449.